



This discussion paper is/has been under review for the journal Atmospheric Chemistry and Physics (ACP). Please refer to the corresponding final paper in ACP if available.

# On the temperature dependence of organic reactivity, nitrogen oxides, ozone production, and the impact of emission controls in San Joaquin Valley California

S. E. Pusede<sup>1</sup>, D. R. Gentner<sup>2</sup>, P. J. Wooldridge<sup>1</sup>, E. C. Browne<sup>1,a</sup>, A. W. Rollins<sup>1,b</sup>, K.-E. Min<sup>3,b</sup>, A. R. Russell<sup>1,c</sup>, J. Thomas<sup>4</sup>, L. Zhang<sup>4</sup>, W. H. Brune<sup>4</sup>, S. B. Henry<sup>5</sup>, J. P. DiGangi<sup>5,d</sup>, F. N. Keutsch<sup>5</sup>, S. A. Harrold<sup>6</sup>, J. A. Thornton<sup>6</sup>, M. R. Beaver<sup>7,e</sup>, J. M. St. Clair<sup>7</sup>, P. O. Wennberg<sup>7</sup>, J. Sanders<sup>8</sup>, X. Ren<sup>8,f</sup>, T. C. VandenBoer<sup>9,g</sup>, M. Z. Markovic<sup>9,b</sup>, A. Guha<sup>10</sup>, R. Weber<sup>10</sup>, A. H. Goldstein<sup>2,10</sup>, and R. C. Cohen<sup>1,3</sup>

<sup>1</sup>Department of Chemistry, University of California Berkeley, Berkeley, California, USA

<sup>2</sup>Department of Civil and Environmental Engineering, University of California Berkeley, Berkeley, California, USA

<sup>3</sup>Department of Earth and Planetary Sciences, University of California Berkeley, Berkeley, California, USA

<sup>4</sup>Department of Meteorology, Pennsylvania State University, University Park, Pennsylvania, USA

<sup>5</sup>Department of Chemistry, University of Wisconsin Madison, Madison, Wisconsin, USA

Title Page

Abstract

Introduction

Conclusions

References

Tables

Figures

◀

▶

◀

▶

Back

Close

Full Screen / Esc

Printer-friendly Version

Interactive Discussion



<sup>6</sup>Department of Atmospheric Sciences, University of Washington, Seattle, Washington, USA

<sup>7</sup>Divisions of Engineering and Applied Science and Geological and Planetary Sciences, California Institute of Technology, Pasadena, California, USA

<sup>8</sup>Rosenstiel School of Marine and Atmospheric Science, University of Miami, Miami, Florida, USA

<sup>9</sup>Department of Chemistry, University of Toronto, Toronto, Ontario, Canada

<sup>10</sup>Department of Environmental Science, Policy, and Management, University of California Berkeley, Berkeley, California, USA

<sup>a</sup>now at: Department of Civil and Environmental Engineering, Massachusetts Institute of Technology, Cambridge, Massachusetts, USA

<sup>b</sup>now at: Earth System Research Laboratory, National Oceanic and Atmospheric Administration and Cooperative Institute for Research in Environmental Sciences, University of Colorado, Boulder, USA

<sup>c</sup>now at: Sonoma Technology, Petaluma, California, USA

<sup>d</sup>now at: Department of Civil and Environmental Engineering, Princeton University, Princeton, New Jersey, USA

<sup>e</sup>now at: National Exposure Research Laboratory, Environmental Protection Agency, Research Triangle Park, North Carolina, USA

<sup>f</sup>now at: Air Resources Laboratory, National Oceanic and Atmospheric Administration, College Park, Maryland, USA

<sup>g</sup>now at: Department of Chemistry and Department of Earth Science, Memorial University of Newfoundland, St. John's, Newfoundland, Canada

Received: 7 October 2013 – Accepted: 17 October 2013 – Published: 1 November 2013

Correspondence to: S. E. Pusede (spusesde@berkeley.edu)

Published by Copernicus Publications on behalf of the European Geosciences Union.

Temperature  
dependent impacts of  
emission controls

S. E. Pusede et al.

Title Page

Abstract

Introduction

Conclusions

References

Tables

Figures

◀

▶

◀

▶

Back

Close

Full Screen / Esc

Printer-friendly Version

Interactive Discussion



## Abstract

The San Joaquin Valley (SJV) experiences some of the worst ozone air quality in the US, frequently exceeding the California 8 h standard of 70.4 ppb. To improve our understanding of trends in the number of ozone violations in the SJV, we analyze observed relationships between organic reactivity, nitrogen oxides ( $\text{NO}_x$ ), and daily maximum temperature in the southern SJV using measurements made as part of California at the Nexus of Air Quality and Climate Change in 2010 (CalNex-SJV). We find the daytime speciated organic reactivity with respect to OH during CalNex-SJV has a temperature-independent portion with molecules typically associated with motor vehicles being the major component. At high temperatures, characteristic of days with high ozone, the largest portion of the total organic reactivity increases exponentially with temperature and is dominated by small, oxygenated organics and molecules that are unidentified. We use this simple temperature classification to consider changes in organic emissions over the last and next decade. With the CalNex-SJV observations as constraints, we examine the sensitivity of ozone production ( $\text{PO}_3$ ) to future  $\text{NO}_x$  and organic reactivity controls. We find that  $\text{PO}_3$  is  $\text{NO}_x$ -limited at all temperatures on weekends and on weekdays when daily maximum temperatures are greater than  $29^\circ\text{C}$ . As a consequence,  $\text{NO}_x$  reductions are the most effective control option for reducing the frequency of future ozone violations in the southern SJV.

## 1 Introduction

California's San Joaquin Valley suffers extremely poor air quality and has so for decades; violations of health-based ozone standards remain frequent despite statewide ozone control measures (Cox et al., 2009). Understanding trends in frequency of these violations requires knowledge of trends in the chemical drivers of ozone production ( $\text{PO}_3$ ) – nitrogen oxides ( $\text{NO}_x \equiv \text{NO} + \text{NO}_2$ ), the reactivity of volatile organic compounds with OH (VOCR), and the production rate of  $\text{HO}_x$  ( $\text{HO}_x \equiv \text{OH} +$

ACPD

13, 28511–28560, 2013

### Temperature dependent impacts of emission controls

S. E. Pusede et al.

Title Page

Abstract

Introduction

Conclusions

References

Tables

Figures

◀

▶

◀

▶

Back

Close

Full Screen / Esc

Printer-friendly Version

Interactive Discussion



HO<sub>2</sub> + RO<sub>2</sub>) radicals – along with trends in the sensitivity of local and regional PO<sub>3</sub> to these parameters. The sequence of ozone forming reactions is generally known; however, determining the response of PO<sub>3</sub> in any location to NO<sub>x</sub> and organic emissions reductions is challenging, as PO<sub>3</sub> is a nonlinear function of each precursor. Meteorological effects impart variability in the number of O<sub>3</sub> violations within a given O<sub>3</sub> season but do not, in the average, impact the inter-annual trends.

In Pusede and Cohen (2012), we examined relationships between nitrogen oxides, the frequency of O<sub>3</sub> exceedances, and temperature, which we used as a proxy for VOCR, over the period 1996 to 2010, inferring from the observed nonlinear nitrogen oxide dependence that chemical production rather than meteorology dominated the statistics of violations in the San Joaquin Valley (SJV). We showed that in the northern SJV (Stockton plume) and central SJV (Fresno plume) PO<sub>3</sub> has largely been sensitive to VOCR and that organic emissions reductions led to decreases in the frequency of O<sub>3</sub> violations. At high temperatures, PO<sub>3</sub> in these plumes is presently NO<sub>x</sub> sensitive. In the southern SJV (Bakersfield plume) at moderate temperatures PO<sub>3</sub> has been sensitive to VOCR for most of the record, with organic emissions controls resulting in fewer annual O<sub>3</sub> violations; simultaneous NO<sub>x</sub> reductions shifted chemistry to peak PO<sub>3</sub> with respect to NO<sub>x</sub> in 2007–2010. At high temperatures, southern SJV PO<sub>3</sub> has been at peak production for most of the last fifteen years, becoming NO<sub>x</sub> sensitive in 2007–2010; at these temperatures, VOCR reductions have made little impact. This temperature dependence in the observed effects of VOCR controls thus suggested two distinct categories of organic reactivity in the Bakersfield plume: one source that had decreased over the last decade and was more important at moderate temperatures and a second source, dominating at high temperatures, that had not substantially changed over the same time period.

During the California at the Nexus of Air Quality and Climate Change experiment (CalNex-SJV), 18 May–29 June 2010, we measured nitrogen oxides, OH reactivity, HO<sub>x</sub> source molecules, and a wide suite of individual volatile organic compounds (VOCs) at the San Joaquin Valley supersite allowing new insight into the production

## Temperature dependent impacts of emission controls

S. E. Pusede et al.

Title Page

Abstract

Introduction

Conclusions

References

Tables

Figures

◀

▶

◀

▶

Back

Close

Full Screen / Esc

Printer-friendly Version

Interactive Discussion



rate of ozone in the region. Here, we use these observations to test the response of  $PO_3$  to variations in temperature, VOCR, and  $NO_x$ . We begin our analysis by describing the temperature dependence of the daytime organic reactivity and categorizing one component of the VOCR that is independent of temperature and a second that increases exponentially with temperature. This simple temperature-response framework allows us to consider how organic emission controls have impacted the total organic reactivity over the last decade and how they will do so over the next ten years. We use the CalNex-SJV observations to constrain a model of instantaneous  $PO_3$  and then to guide our thinking about the frequency of  $O_3$  violations in the complete 2010  $O_3$  season. We test various emissions reductions scenarios and show both the magnitude and sign of the effects of controls on emissions are temperature dependent.

## 2 Chemical production of $O_3$

### 2.1 $PO_3$ reaction sequence

$PO_3$  is initiated by the oxidation of gas-phase organic molecules. During the daytime, this usually involves reaction with the hydroxyl radical (OH) leading to formation of an alkyl radical (R), which immediately reacts with  $O_2$  to form a peroxy radical ( $RO_2$ ). In the typical chain-propagating branch of this sequence,  $RO_2$  reacts with NO to form an alkoxy radical (RO) and  $NO_2$ . In the presence of  $O_2$ , the RO leads to formation of  $HO_2$  and an aldehyde or ketone. The  $HO_2$  in turn reacts with NO to form a second  $NO_2$  molecule and regenerate OH. Hence Reactions (R1)–(R5) are catalytic, being  $HO_x$  neutral while converting NO to  $NO_2$ .

## Temperature dependent impacts of emission controls

S. E. Pusede et al.

Title Page

Abstract

Introduction

Conclusions

References

Tables

Figures

⏪

⏩

◀

▶

Back

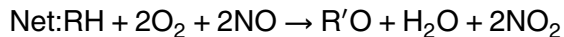
Close

Full Screen / Esc

Printer-friendly Version

Interactive Discussion





The importance of any individual VOC in the HO<sub>x</sub> cycle depends on its reaction rate with OH (*k*<sub>OH</sub>). The rate at which a single organic species reacts with OH is defined as  $\text{VOCR}_i \equiv k_{\text{OH}+\text{VOC}_i}[\text{VOC}_i]$  with units of s<sup>-1</sup>; for the entire VOC mixture, we define the total organic reactivity (VOCR). Throughout this paper we use  $\sum_i \text{VOCR}_i$  to refer to the reactivity summed from individually measured compounds; we use VOCR both generally and to refer to the VOCR obtained from direct measurements of the total OH reactivity. In the continental boundary layer, representative daytime VOCR values are: 7–12 s<sup>-1</sup> in suburban Nashville, Tennessee (Kovacs et al., 2003); 10–30 s<sup>-1</sup> in the polluted megacity Beijing (Lou et al., 2010); and 1–13 s<sup>-1</sup> at a rural forest site in Michigan and covarying with daytime temperatures of 10–27 °C (Di Carlo et al., 2004).

The photolysis of NO<sub>2</sub> gives NO (NO<sub>x</sub> is conserved on timescales of the interconversion between NO and NO<sub>2</sub>) and a ground-state oxygen atom, which rapidly combines with O<sub>2</sub> to form O<sub>3</sub> (Reactions R6 and R7).



For a typical organic molecule, used as a basis for Reactions (R1)–(R7), the net reaction yields two O<sub>3</sub> from one OH reaction. Variations in this mechanism include compounds that produce one (e.g., carbon monoxide), three (e.g., acetaldehyde), or more  
25 O<sub>3</sub> molecules.

## Temperature dependent impacts of emission controls

S. E. Pusede et al.

[Title Page](#)[Abstract](#)[Introduction](#)[Conclusions](#)[References](#)[Tables](#)[Figures](#)[◀](#)[▶](#)[◀](#)[▶](#)[Back](#)[Close](#)[Full Screen / Esc](#)[Printer-friendly Version](#)[Interactive Discussion](#)

While  $PO_3$  radical chemistry is propagated by reactions involving  $HO_x$  and  $NO_x$ , it is terminated by reactions between the same species (Reactions R8–R11 and R3'). Herein arises the non-linear dependence of  $PO_3$  on  $NO_x$  and VOCR.



Reaction (R3') is the minor channel of Reaction (R3) and, depending on the identity of the VOC, its branching,  $k_{R3'}/(k_{R3} + k_{R3'})$ , is 0–35%. Ambient air organic mixtures are observed to have average Reaction (R3') branching ratios in the range of 2–8% (Perring et al., 2013).

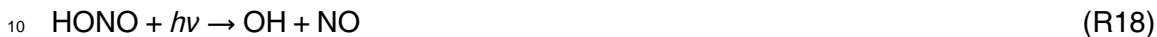
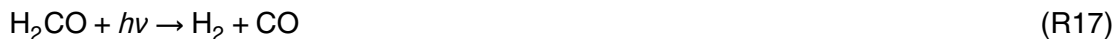
15 At low  $NO_x$ , increasing NO drives Reactions (R3) and (R5), and therefore the oxidation of VOCs and  $PO_3$ . Chemistry in this regime is  $NO_x$ -limited and increases in VOCR have little effect on  $PO_3$ . At higher  $NO_x$  levels,  $NO_2$  begins to outcompete organics for OH (Reaction R12) and the  $PO_3$  rate slows. Chemistry here is VOC-limited (also known as  $NO_x$ -suppressed or  $NO_x$ -saturated). At a given VOCR,  $PO_3$  is maximized  
20 at the transition point between the  $NO_x$ - and VOC-limited regimes. At peak  $PO_3$ , the production of alkyl nitrates by Reaction (R3') and peroxy nitrates also reach a peak. The formation of these nitrates is important to the absolute  $PO_3$  but has little effect on  $PO_3$ 's functional form (Farmer et al., 2011; Perring et al., 2013). When chemistry is VOC-limited, the impact of increasing the VOCR is twofold: (a) it increases the mag-  
25 nitude of  $PO_3$  and (b) it shifts the position of peak  $PO_3$  to higher  $NO_x$ . Thus, the  $NO_x$  concentration at which  $PO_3$  transitions from  $NO_x$ -limited to VOC-limited is VOCR dependent – a dependence that has important implications in the design of organic and  $NO_x$  emission control strategies.

## Temperature dependent impacts of emission controls

S. E. Pusede et al.

[Title Page](#)[Abstract](#)[Introduction](#)[Conclusions](#)[References](#)[Tables](#)[Figures](#)[◀](#)[▶](#)[◀](#)[▶](#)[Back](#)[Close](#)[Full Screen / Esc](#)[Printer-friendly Version](#)[Interactive Discussion](#)

The production of new HO<sub>x</sub> molecules (*PHO<sub>x</sub>*) results primarily from the photolysis of O<sub>3</sub> (Reactions R13 and R14), formaldehyde (H<sub>2</sub>CO) (Reaction R16), nitrous acid (HONO)(Reaction R18), to a smaller extent hydrogen peroxide (H<sub>2</sub>O<sub>2</sub>) (Reaction R19), and chemical reactions between O<sub>3</sub> and alkenes.



At VOC-limited and peak *PO*<sub>3</sub>, an increase in *PHO<sub>x</sub>* enhances *PO*<sub>3</sub> nearly one to one. At NO<sub>x</sub>-limited *PO*<sub>3</sub>, *PO*<sub>3</sub> scales approximately as  $2k_{\text{HO}_2+\text{NO}} \left( \frac{\text{PHO}_x}{k_{\text{HO}_2+\text{HO}_2}} \right)^{\frac{1}{2}} [\text{NO}]$ . Decreasing *PHO<sub>x</sub>* also shifts peak *PO*<sub>3</sub> to lower NO<sub>x</sub> but to a smaller extent than the equivalent shift from decreasing VOCR. For example, at 10 s<sup>-1</sup> VOCR and 1 ppts<sup>-1</sup> *PHO<sub>x</sub>*, a 50 % reduction in VOCR shifts peak *PO*<sub>3</sub> to ~ 30 % lower NO<sub>x</sub> while the same *PHO<sub>x</sub>* reduction has half the effect. The photolysis of nitrile chloride (CINO<sub>2</sub>) also initiates radical chemistry in the early morning (e.g., Osthoff et al., 2008; Thornton et al., 2010; Mielke et al., 2011). CINO<sub>2</sub> is not included in our model (described below) as we focus on daytime chemistry from 10 a.m.–2 p.m. when CINO<sub>2</sub> is no longer present in relevant amounts.

## 2.2 Analytical model of *PO*<sub>3</sub>

We compute *PO*<sub>3</sub> with an analytical model similar to that described by Murphy et al. (2007) and Farmer et al. (2011). We summarize our specific formulation here.

### Temperature dependent impacts of emission controls

S. E. Pusede et al.

Title Page

Abstract

Introduction

Conclusions

References

Tables

Figures

◀

▶

◀

▶

Back

Close

Full Screen / Esc

Printer-friendly Version

Interactive Discussion





This calculation assumes HO<sub>x</sub> is in steady state (Eq. 1).

$$PHO_x = k_{HO_2+HO_2}[HO_2]^2 + 2k_{HO_2+RO_2}[HO_2][RO_2] + 2k_{RO_2+RO_2}[RO_2]^2 + k_{NO_2+OH}[OH][NO_2] + \alpha k_{NO+RO_2}[NO][RO_2] \quad (1)$$

5 During daytime Eq. (1) is an accurate approximation, as radical propagation (Reactions R1–R5) dominates termination (Reactions R8–R12 and R3'). RO<sub>2</sub> production approximately equals that of HO<sub>2</sub> and, also by the steady–state relation, RO<sub>2</sub> loss. This simplifying framework gives Eq. (2) for both RO<sub>2</sub> and HO<sub>2</sub> with  $\alpha$  as the alkyl nitrate branching ratio.

$$10 [RO_2] \sim [HO_2] = \frac{VOCR[OH]}{(1 - \alpha)k_{NO+RO_2}[NO]} \quad (2)$$

Peroxy nitrates are treated to be in thermal equilibrium with NO<sub>2</sub> + acyl peroxy radicals and therefore do not contribute to net radical formation.

Equations (1) and (2) are combined to solve for OH (Eq. 3), with the coefficients  $a$ ,  $b$ , and  $c$  given by Eqs. (4)–(6), respectively.

$$15 [OH] = \frac{-b + \sqrt{b^2 - 4ac}}{2a} \quad (3)$$

$$a = (2k_{HO_2+HO_2} + 2k_{HO_2+RO_2} + 2k_{RO_2+RO_2}) \left( \frac{VOCR}{(1 - \alpha)k_{NO+RO_2}[NO]} \right)^2 \quad (4)$$

$$b = k_{NO_2+OH}[NO_2] + \frac{\alpha k_{NO+RO_2}[NO_2]VOCR}{(1 - \alpha)k_{NO+RO_2}} \quad (5)$$

$$c = -PHO_x \quad (6)$$

20 Solving for OH and then HO<sub>2</sub> gives  $PO_3 = (k_{NO+HO_2} + k_{NO+RO_2})[NO][HO_2]$  when  $\alpha \ll 1$ .  
28519

Temperature dependent impacts of emission controls

S. E. Pusede et al.

Title Page

Abstract

Introduction

Conclusions

References

Tables

Figures

◀

▶

◀

▶

Back

Close

Full Screen / Esc

Printer-friendly Version

Interactive Discussion



The observational inputs to the calculation are NO and NO<sub>2</sub>, the total VOCR, PHO<sub>x</sub>, α, and temperature. In our analysis, VOCR, PHO<sub>x</sub>, and the NO to NO<sub>x</sub> ratio are fit as exponential functions of temperature and we use these fits to constrain the model; VOCR, PHO<sub>x</sub>, and α are discussed below.

Total VOCR is equal to the measured OH reactivity minus the OH reactivities of NO, NO<sub>2</sub>, HONO, HNO<sub>3</sub>, ammonia (NH<sub>3</sub>), and sulfur dioxide (SO<sub>2</sub>).

PHO<sub>x</sub> is the summed HO<sub>x</sub> production rates of O<sub>3</sub>, H<sub>2</sub>CO, HONO, and H<sub>2</sub>O<sub>2</sub> photolysis and O<sub>3</sub> reactions with alkenes. Noontime HONO concentrations during CalNex-SJV were between 30–250 ppt (Ren et al., 2011; VandenBoer et al., 2013) making HONO an important radical source throughout the day. H<sub>2</sub>O<sub>2</sub> photolysis (1 %) and O<sub>3</sub> + alkene reactions (7 %) are less important to the daytime total. Photolysis frequencies are computed with the TUV calculator ([http://cprm.acd.ucar.edu/Models/TUV/Interactive\\_TUV](http://cprm.acd.ucar.edu/Models/TUV/Interactive_TUV)) (Madronich, 1987) at 1 h resolution for a clear sky day (7 June 2010) and used to scale the 1 min measured photosynthetically active radiation to capture changes with cloud cover. The O<sub>3</sub> optical depth used is 300 Dobson units, measured by OMI on 7 June 2010 (<http://www.temis.nl/protocols/O3total.html>) (Veefkind et al., 2006). The measurement altitude of the CalNex-SJV site is 0.14 km (a.s.l.). The surface albedo, 0.8, was determined using the MODIS 16 day 500 m product in band 3 (459–479 nm) for 18 June 2010. The product was reprojected at a fine resolution (0.001° ~ 10 m) for the CalNex-SJV site-specific surface reflectivity. The photolysis rates were reduced by 10 % so that calculated PHO<sub>x</sub> ~ LHO<sub>x</sub>. PHO<sub>x</sub> is averaged over the 10 a.m.–2 p.m. LT window.

An effective α value is inferred from observations of O<sub>x</sub> (O<sub>x</sub> ≡ O<sub>3</sub> + NO<sub>2</sub>) and total alkyl nitrates (ΣANs) as two divided by the slope of their correlation (Perring et al., 2013). Deriving α this way treats O<sub>x</sub> and ΣAN concentrations as proxies for their respective production rates and assumes that, on average, two O<sub>3</sub> are produced per unit VOCR. During CalNex-SJV the daily average α is 2–3 % (2σ) and we use 2.5 % as a constant in our calculation. The NO<sub>x</sub> value at peak PO<sub>3</sub> is sensitive to α, where a lower α value

## Temperature dependent impacts of emission controls

S. E. Pusede et al.

Title Page

Abstract

Introduction

Conclusions

References

Tables

Figures

◀

▶

◀

▶

Back

Close

Full Screen / Esc

Printer-friendly Version

Interactive Discussion



gives  $\partial PO_3/\partial NO_x$  equal to zero at higher  $NO_x$ . Variability in  $\alpha$  of  $\pm 0.5\%$  is not large enough to affect our results.

### 3 Observations

#### 3.1 CalNex-SJV measurements

5 California at the Nexus of Air Quality and Climate Change (CalNex) was a multi-site, multi-platform field intensive that took place in the spring of 2010 across California (Ryerson et al., 2013). The San Joaquin Valley supersite (CalNex-SJV) was located at the University of California Extension-Kern County (35.346° N, 118.965° W). Daytime (10 a.m.–2 p.m. LT) winds to the site were consistently from the northwest and at  
10 on average  $2\text{--}3\text{ m s}^{-1}$  ( $\sim 1\sigma$ ). The CalNex-SJV site was 6 km southeast of downtown Bakersfield and typically less than an hour downwind.

Continuous in-situ observations of over 10 VOCs,  $H_2CO$ , peroxy acyl nitrate (PAN), peroxypropionyl nitrate (PPN),  $C_1\text{--}C_3$  organic acids, glyoxal, carbon monoxide (CO), methane ( $CH_4$ ), OH reactivity, NO,  $NO_2$ ,  $HNO_3$ ,  $NH_3$ ,  $SO_2$ ,  $\Sigma ANs$ ,  $O_3$ ,  $H_2O_2$ , and meteorological parameters (e.g., temperature, relative humidity, and photosynthetically active radiation) were collected from 18 May to 29 June 2010 atop an 18 m walk-up tower. HONO was measured at a lower tower level 15.3 m above ground. Table A1 lists the measurement uncertainty, instrumental technique, and associated reference(s) for each species used in this analysis. All observations are at  
15 at 1 min time resolution with the following exceptions: VOCs (1 h),  $NH_3$  and  $SO_2$  (1 h), OH reactivity (10 min), and HONO (2 min) (<http://www.esrl.noaa.gov/csd/groups/csd/7/measurements/2010calnex/>). Acetaldehyde, the first-generation isoprene oxidation product methyl vinyl ketone (MVK), ethane, and benzene were not measured. Their concentrations were calculated via relationships with observed species (see Appendix A1 for details).  
20  
25

Title Page

Abstract

Introduction

Conclusions

References

Tables

Figures

◀

▶

◀

▶

Back

Close

Full Screen / Esc

Printer-friendly Version

Interactive Discussion







In Fig. 1 we show that the daily average  $\sum_i \text{VOCR}_i$  of certain anthropogenic VOCs (AVOCs) and CO is independent of temperature; the reactivities of C<sub>1</sub>–C<sub>2</sub> aldehydes, C<sub>1</sub>–C<sub>3</sub> alcohols, known-biogenic VOCs, CH<sub>4</sub>, a subset of alkanes and C<sub>1</sub>–C<sub>3</sub> organic acids increase exponentially with increasing temperature. The data points, summarized in Fig. 1, are given in Fig. A1. We find that at low and moderate temperatures, temperature-independent AVOCs and CO represent the largest portion of  $\sum_i \text{VOCR}_i$ . At high temperatures, the small oxygenates, H<sub>2</sub>CO, acetaldehyde, and C<sub>1</sub>–C<sub>3</sub> alcohols, dominate. The known-biogenic source is only a minor contributor to VOCR in the southern SJV even at the highest temperatures (10 % of  $\sum_i \text{VOCR}_i$  and 5 % of VOCR at 36.4 °C).

In Fig. 2  $\sum_i \text{VOCR}_i$  and VOCR are organized according to temperature dependence: temperature-independent  $\sum_i \text{VOCR}_i$  (blue), known temperature-dependent  $\sum_i \text{VOCR}_i$  (yellow), and unknown temperature-dependent reactivity (green). The temperature-independent  $\sum_i \text{VOCR}_i$  has a mean value of 2.1 s<sup>-1</sup>; it is equal to the sum of temperature-independent AVOCs, CO, 0.2 s<sup>-1</sup> H<sub>2</sub>CO, and 0.15 s<sup>-1</sup> temperature-dependent alkane  $\sum_i \text{VOCR}_i$ . Light-duty vehicles are known to emit these molecules, the largest portion of this vehicular source (70–90 %) being temperature-independent tailpipe emissions (Pierson et al., 1999; Rubin et al., 2006; Gentner et al., 2009). An aside: the temperature-dependent alkane  $\sum_i \text{VOCR}_i$  category has been further divided into temperature-dependent and temperature-independent components, henceforth associating the  $\sim y$ -intercept value of 0.15 s<sup>-1</sup> (Fig. 1 orange line) with vehicle emissions (i.e. temperature-independent  $\sum_i \text{VOCR}_i$ ) and the remaining reactivity, having a distinctly temperature-driven source, with evaporative emissions from gasoline vehicles and fugitive emissions from petroleum operations (Gentner et al., 2013a).

oxidation products of these emissions, et alia (Table A2). Isoprene and monoterpenes are emitted from different plant species, are transported to the CalNex-SJV site from different distances, and exhibit unique light, humidity, and (very high) temperature dependence (Guenther et al., 1993).

## Temperature dependent impacts of emission controls

S. E. Pusede et al.

Title Page

Abstract

Introduction

Conclusions

References

Tables

Figures

◀

▶

◀

▶

Back

Close

Full Screen / Esc

Printer-friendly Version

Interactive Discussion



**Temperature  
dependent impacts of  
emission controls**

S. E. Pusede et al.

Title Page

Abstract

Introduction

Conclusions

References

Tables

Figures

◀

▶

◀

▶

Back

Close

Full Screen / Esc

Printer-friendly Version

Interactive Discussion

The temperature-dependent  $\sum_i \text{VOCR}_i$  and temperature-dependent VOCR, the latter defined here as the measured OH reactivity minus the temperature-independent  $\sum_i \text{VOCR}_i$  and OH reactivities of NO, NO<sub>2</sub>, HONO, HNO<sub>3</sub>, NH<sub>3</sub>, and SO<sub>2</sub>, are also shown. A comparison of these data indicates a portion of the reactivity is unaccounted for by VOC observations. This unknown reactivity is temperature dependent, increasing from ~ zero at low temperatures to ~ 5 s<sup>-1</sup> at high temperatures. Our estimate for VOCR<sub>acetaldehyde</sub> is uncertain (Appendix A1). We include VOCR<sub>acetaldehyde</sub> in Figs. 1 and 2, as we are interested in the magnitude of the unknown as opposed to the unmeasured VOCR.

Identifying what molecules/sources are responsible for the unknown organic activity is not the aim of this work but we are able to establish the temperature response of the unknown source(s). We note that it has been previously speculated that a missing source of VOCR is important when O<sub>3</sub> is high in the SJV (Steiner et al., 2008; Hu et al., 2012; Pusede and Cohen, 2012). Organic sources with this temperature dependence include molecules with emissions rates controlled by their vapor pressures, biogenic VOCs from forests (e.g., Guenther et al., 1993) and cultivated fields, as well as the oxidation products of these emissions (e.g., Huisman et al., 2011; Mao et al., 2012). In the southern SJV, known organic sources likely to be temperature dependent are diverse and are arranged in an overlapping patchwork surrounding the CalNex-SJV site. These sources include: emissions from dairy wastes (e.g., Shaw et al., 2007; Gentner et al., 2013a) and animal feeds (Alanis et al., 2010; Howard et al., 2010a, b; Malkina et al., 2011); biogenic emissions from crops (e.g., Ormeño et al., 2010; Fares et al., 2011, 2012; Gentner et al., 2013b) and forests in the adjacent Sierra Nevada foothills (e.g., Schade and Goldstein, 2001; LaFranchi et al., 2011; Park et al., 2013); and the evaporative emissions of oil and gas extraction activities, as suggested by our observation of temperature-dependent light alkane mixing ratios.

In Pusede and Cohen (2012) – using temperature as a proxy for VOCR – we showed that the frequency of 8 h O<sub>3</sub> violations in Bakersfield and the southern SJV region at moderate temperatures fell substantially from 1999–2010 because of VOCR reduc-



## Temperature dependent impacts of emission controls

S. E. Pusede et al.

Title Page

Abstract

Introduction

Conclusions

References

Tables

Figures

⏪

⏩

◀

▶

Back

Close

Full Screen / Esc

Printer-friendly Version

Interactive Discussion



tions; the same was not true at high temperatures and we concluded that there were two reasons for this.<sup>2</sup> (1) At moderate temperatures O<sub>3</sub> chemistry was VOC-limited for most of the record and, as such, the exceedance frequency was sensitive to changes in VOCR. At high temperatures, O<sub>3</sub> chemistry was near peak PO<sub>3</sub>, and recently (2007–2010) NO<sub>x</sub>-limited on weekends, and thus less sensitive to VOCR decreases. (2) There were two distinct categories of organic reactivity in the southern SJV – one source that had decreased over the last decade and was more important at moderate temperatures and a second source that dominated at high temperatures and had not substantially changed.

In light of the CalNex-SJV  $\sum_i \text{VOCR}_i$  and VOCR observations and well-documented efforts to control motor vehicle emissions (e.g., Kirchstetter et al., 1999a, 1999b; Parrish et al., 2002; Harley et al., 2006; Parrish, 2006; Bishop and Stedman, 2008) we speculate that it is the temperature-independent reactivity that has decreased over the last decade. At the same time, we know of no deliberate attempt to control the molecules dominating the reactivity at high temperatures – small aldehydes, alcohols, and the unknown VOCR. It is therefore likely that the temperature-independent  $\sum_i \text{VOCR}_i$  of 2.1 s<sup>-1</sup> is the endpoint of long-term efforts at organic emissions reductions.

Routine summertime VOC canister sampling in the southern SJV (Appendix B) suggests a decrease of  $\sim 6\% \text{ yr}^{-1}$  in temperature-independent emissions. In what follows, we use this  $-6\% \text{ yr}^{-1}$  rate in the temperature-independent  $\sum_i \text{VOCR}_i$  and assume no change in temperature-dependent emissions to illustrate the effects of VOC controls from 2000 to 2010 on the total VOCR (Fig. 3). We show that over the last decade the impact of reductions on the total VOCR (black) have been greatest at low temperatures (5–35%) and smallest at high temperatures (20–15%). We show the predicted percent change in total VOCR in the next decade, assuming the temperature-independent  $\sum_i \text{VOCR}_i$  continues to decrease at the same rate (periwinkle). Again, the impacts are

<sup>2</sup>Pusede and Cohen (2012) did not include an analysis at low temperatures because exceedances at these temperatures were infrequent or did not occur.



largest at low temperatures (55–25%) and smallest at high temperatures (15–10%). An interesting feature of Fig. 3 is that the temperature dependence becomes more prominent in the future as the temperature-independent component declines.

## 4.2 Combined $\text{NO}_x$ and temperature dependence

$\text{NO}_x$  decreases by  $\sim 60\%$  from weekdays (5.3 ppb) to weekends (2.3 ppb) and is observed to be temperature independent (Fig. 4a). In Fig. 4b and we combine relationships between temperature, total VOCR, and  $\text{NO}_x$  (as  $\text{NO}_x\text{R} \equiv \text{NO}_x$  reactivity with OH). On weekends, VOCR/ $\text{NO}_x\text{R}$  is more than double that on weekdays. On both weekdays and weekends the observed VOCR/ $\text{NO}_x\text{R}$  increases with temperature by more than a factor of ten across the temperature range of 15–40°C.

Figure 4b suggests that the combined  $\text{NO}_x$  and VOCR relationships with temperature impart a dependence on temperature of the sensitivity of  $\text{PO}_3$  to its precursor emissions. To investigate this, we calculate  $\text{PO}_3$  as described in Sect. 2.2 using the temperature relationships of VOCR,  $\text{PHO}_x$ , and  $\text{NO}/\text{NO}_x$  observed during CalNex-SJV (Fig. 5a–c).  $\text{PHO}_x$  increases with increasing temperature. This temperature dependence is driven by the  $\text{HO}_x$  source molecules  $\text{O}_3$  (34% of  $\text{PHO}_x$ ), HONO (32% of  $\text{PHO}_x$ ), and  $\text{H}_2\text{CO}$  (26% of  $\text{PHO}_x$ ) each increasing with increasing temperature so that the relative contributions are similar across the 15–40°C range.  $\text{NO}/\text{NO}_x$  decreases with increasing temperature, this ratio being set by the  $\text{O}_3$  concentration (Fig. 5d). For context, we also show the daily average (10 a.m.–2 p.m. LT)  $\text{O}_3$  during CalNex-SJV (magenta) and over the entire 2010  $\text{O}_3$  season (1 May–31 October) (gray). Fitting the 2010  $\text{O}_3$  (gray) vs. daily maximum temperature to a line (not shown) yields a weekday slope that is 28% steeper on weekdays than on weekends.

Large changes in  $\text{NO}_x$ , like those occurring weekday to weekend, impact OH concentrations; this change in OH has a feedback on VOCR and  $\text{NO}_x$ . Higher OH reduces total VOCR, as oxidized organic molecules are usually less reactive than their parent VOC. OH has the same functional form as  $\text{PO}_3$  and, analogously, is least responsive to changes in  $\text{NO}_x$  near peak  $\text{PO}_3$ . Higher average weekday  $\text{O}_3$  (gray) at

### Temperature dependent impacts of emission controls

S. E. Pusede et al.

Title Page

Abstract

Introduction

Conclusions

References

Tables

Figures

◀

▶

◀

▶

Back

Close

Full Screen / Esc

Printer-friendly Version

Interactive Discussion



## Temperature dependent impacts of emission controls

S. E. Pusede et al.

Title Page

Abstract

Introduction

Conclusions

References

Tables

Figures

◀

▶

◀

▶

Back

Close

Full Screen / Esc

Printer-friendly Version

Interactive Discussion



high temperatures indicates chemistry is  $\text{NO}_x$ -limited (a point examined in detail in Sect. 4.3). Equal weekday-to-weekend percent decreases in OH occur alongside decreases in  $\text{PO}_3$  and an equivalent reduction in the OH-reaction removal rate of organic emissions is implied; however, enhanced weekend VOCCR at high temperatures is not observed (Fig. 5a). A compensating increase in organic emissions on weekends is unlikely, as high-temperature reactivity is dominated by molecules with emissions rates controlled by temperature and not by human activity (Sect. 4.1). Temperature-independent  $\sum_i \text{VOCCR}_i$  is also invariant with day of week (not shown). We are not able to definitively explain the absence of a day-of-week dependence of VOCCR but suggest it is a combined effect of (a) the specific VOCCR mixture in the southern SJV, (b) the limited statistics, and (c) the variability with temperature.

### 4.3 Ozone production rates and the impacts of emissions controls

Ozone production rates calculated using Eqs. (1)–(6) are useful for interpreting the observed frequency of  $\text{O}_3$  violations and the sensitivity of  $\text{PO}_3$  chemistry to emissions changes. In Fig. 6 we map  $\text{PO}_3$  ( $\text{ppbh}^{-1}$ ) as a function of  $\text{NO}_x$  and temperature, with the latter as a surrogate for VOCCR (the fit from Fig. 5a). The average weekday (solid line) and weekend (dashed line)  $\text{NO}_x$  mixing ratios are shown. In Table 1 we report  $\text{PO}_3$  at average low (purple), moderate (blue), and high (red) temperatures. Note the exponential form of the temperature dependence of the transition point between  $\text{NO}_x$ -limited and VOC-limited regimes. At low temperatures (the 2010 average),  $\text{PO}_3$  is VOC-limited and increases weekday to weekend. At moderate temperatures, weekday  $\text{PO}_3$  is VOC-limited (1 ppb  $\text{NO}_x$  right of peak  $\text{PO}_3$ ) but decreases by 17% on weekends. At high temperatures,  $\text{PO}_3$  is at the peak with respect to  $\text{NO}_x$  on weekdays and decreases by 42% on weekends, when  $\text{PO}_3$  is  $\text{NO}_x$ -limited.

We compare the results of our CalNex-SJV parameterized  $\text{PO}_3$  calculation to the complete Bakersfield 2010  $\text{O}_3$  record (Table 1). At low temperatures, there were no exceedances of the 8 h  $\text{O}_3$  standard on either weekdays or weekends. At moder-

## Temperature dependent impacts of emission controls

S. E. Pusede et al.

Title Page

Abstract

Introduction

Conclusions

References

Tables

Figures

◀

▶

◀

▶

Back

Close

Full Screen / Esc

Printer-friendly Version

Interactive Discussion



ate temperatures there were  $0.22 \pm 0.09$  exceedances  $\text{day}^{-1}$  on weekdays and  $0.25 \pm 0.11$  exceedances  $\text{day}^{-1}$  on weekends. This is a 14% increase in the frequency of  $\text{O}_3$  exceedances weekday to weekend. At high temperatures there were  $0.76 \pm 0.07$  exceedances  $\text{day}^{-1}$  on weekdays and  $0.43 \pm 0.10$  exceedances  $\text{day}^{-1}$  on weekends, a 43% reduction in the frequency of violations in response the changes in emissions, particularly the 60%  $\text{NO}_x$  reduction on weekends. Uncertainties in exceedance frequency are treated as counting errors as  $0.5(N)^{1/2}/N$ , with  $N$  being the total numbers of days in that day-of-week and temperature bin. We see that at high temperatures, the weekday-to-weekend change in exceedance probability (43%) is comparable to the 42% decrease in calculated  $PO_3$ .

To make sense of the comparison at moderate temperatures and between temperature regimes requires consideration of an additional variable – that the  $\text{O}_3$  concentration is an integrated function of  $PO_3$  across the span of an urban plume. In Fig. 6, placing  $\text{NO}_x$  on the  $y$  axis illustrates this: directly upwind of the CalNex site was the Bakersfield city center, where  $\text{NO}_x$  emissions are higher and, according to Fig. 6,  $PO_3$  is higher as well. The CalNex-SJV site was located at the plume edge (OMI satellite imagery) where gradients are steep and the upwind impact large. At high temperatures, because weekday chemistry is near peak  $PO_3$  and because peak  $PO_3$  spans the widest range in  $\text{NO}_x$  at the highest VOCCR, upwind and local  $\text{NO}_x$  control over production are similar, as such,  $PO_3$  and the exceedance frequency are in close agreement. At moderate temperatures, we compute that a 60% decrease in  $\text{NO}_x$  is enough to transition the calculation of instantaneous  $PO_3$  to  $\text{NO}_x$ -limited chemistry at the CalNex-SJV site but the exceedance data suggest this not true upwind or for the integrated  $PO_3$ . Likewise, violations are approximately 40% more frequent at the equivalent  $PO_3$  at high temperatures than at moderate temperatures.

We use our constrained  $PO_3$  calculation to test the effects of possible controls on emissions (Fig. 7). We consider the following three strategies:  $-50\%$   $\text{NO}_x$  (panels a and d),  $-50\%$  temperature-independent  $\sum_i \text{VOCCR}_i$  (panels b and e), and  $-50\%$   $\text{NO}_x$  and  $-50\%$  temperature-independent  $\sum_i \text{VOCCR}_i$  (panels c and f). If temperature-



**Temperature  
dependent impacts of  
emission controls**

S. E. Pusede et al.

Title Page

Abstract

Introduction

Conclusions

References

Tables

Figures

◀

▶

◀

▶

Back

Close

Full Screen / Esc

Printer-friendly Version

Interactive Discussion



will be further attenuated alongside co-occurring  $\text{NO}_x$  decreases. A 50% reduction in the temperature-dependent  $\sum_i \text{VOCR}_i$  on top of the 50% reduction in temperature-independent  $\sum_i \text{VOCR}_i$  (not shown) reduces high-temperature (36.4 °C)  $\text{PO}_3$  by an additional 6% on weekdays and 1% on weekends. A 50% reduction in the total VOCR, including reactivity from unknown molecules, decreases  $\text{PO}_3$  at high temperatures by 25% and 6% on weekdays and weekends, respectively. However, VOCR reductions of equal effect to equivalent  $\text{NO}_x$  controls require development of new approaches, as existing controls do not target the molecules dominating the reactivity at high temperatures and existing measurement networks do not observe them. Planning and executing reductions in this VOCR will likely require years of effort – a time period during which  $\text{NO}_x$  controls on diesel trucks will be fully implemented and other strategies for  $\text{NO}_x$  reduction could be developed with knowledge of how to monitor their success.

One consequence of the local photochemistry moving to a  $\text{NO}_x$ -limited regime is that  $\text{PO}_3$ 's temperature dependence will diminish, as temperature-driven increases in VOCR will not increase  $\text{PO}_3$  (compare Fig. 7a's black solid and brown dashed lines). In the future we expect less variability in  $\text{PO}_3$  and by extension less variability in the frequency of  $\text{O}_3$  exceedances with temperature.

## 5 Summary

Using CalNex-SJV observations of organic molecules, OH reactivity,  $\text{O}_3$ , and nitrogen oxides we describe relationships between temperature,  $\sum_i \text{VOCR}_i$ , VOCR,  $\text{NO}_x$ , and  $\text{PO}_3$ . We find the  $\sum_i \text{VOCR}_i$  in the southern San Joaquin Valley (SJV) has a temperature-independent component with a reactivity of  $2.1 \text{ s}^{-1}$  and a temperature-dependent component that increases exponentially from  $0 \text{ s}^{-1}$  at  $< 25 \text{ °C}$  to  $\sim 5 \text{ s}^{-1}$  at high temperatures. The temperature-independent  $\sum_i \text{VOCR}_i$  is composed of organic molecules associated with motor vehicle emissions. The known molecules contributing to the temperature-dependent VOCR are dominated by small aldehydes and alcohols; however, unidentified molecules are the largest source of reactivity at high tempera-

tures. The OH reactivity of  $\text{NO}_x$  is temperature independent and decreases by  $\sim 60\%$  from weekdays to weekends.

We compute  $PO_3$  using an analytical model constrained by the CalNex-SJV measurements. In response to the observed  $\sim 60\%$   $\text{NO}_x$  decreases (at constant VO $CR_i$ ) occurring on weekends, we calculate that  $PO_3$  increases at low temperatures, decreases by 17% at moderate temperatures, and decreases by 42% at high temperatures (Fig. 6). We show consistency between weekday-to-weekend percent changes in the frequency of exceedances of the California 8 h  $O_3$  standard (70.4 ppb) and the constrained model predictions suggesting the results of this short-term field experiment, viewed in the framework of temperature, give insight into the entire  $O_3$  season in the southern SJV.

Using this same  $PO_3$  model we estimate the effects of possible emissions control scenarios and show the impacts are variable with temperature in both sign and magnitude. We conclude that  $\text{NO}_x$  reductions will be immediately and incrementally productive at reducing  $PO_3$  on weekends at moderate temperatures and on both weekdays and weekends at high temperatures, which is when exceedances are most frequent. Reductions of the temperature-independent organic reactivity will be effective at low temperatures only; however, there were no violations of the California 8 h  $O_3$  standard in 2010 at these temperatures. The impact of reductions of temperature-independent VOC emissions on  $O_3$  violations at moderate and high temperatures will be further diminished with co-occurring  $\text{NO}_x$  decreases.

## Appendix A

### CalNex-SJV measurements and $\sum_i \text{VOCR}_i$

Table A1 lists each observation/class of observed compounds, the measurement uncertainty, analytical technique, and associated reference included in our analysis.

ACPD

13, 28511–28560, 2013

## Temperature dependent impacts of emission controls

S. E. Pusede et al.

Title Page

Abstract

Introduction

Conclusions

References

Tables

Figures

⏪

⏩

◀

▶

Back

Close

Full Screen / Esc

Printer-friendly Version

Interactive Discussion



Temperature  
dependent impacts of  
emission controls

S. E. Pusede et al.

Title Page

Abstract

Introduction

Conclusions

References

Tables

Figures

◀

▶

◀

▶

Back

Close

Full Screen / Esc

Printer-friendly Version

Interactive Discussion

In Fig. A1 we show the daily averaged (10 a.m.–2 p.m. LT)  $\sum_i \text{VOCR}_i$  vs. daily maximum temperature for  $\text{C}_1$ – $\text{C}_2$  small aldehydes (panel a),  $\text{C}_1$ – $\text{C}_3$  alcohols (panel b), known-biogenic VOCs (panel c),  $\text{CH}_4$  (panel d), temperature-dependent alkanes (generally those with  $< \text{C}_{10}$ ) (panel e),  $\text{C}_1$ – $\text{C}_3$  organic acids (panel f), the sum of all alkanes, alkenes, aromatics, and carbonyls observed to be independent of temperature (panel g), and CO (panel h). In panels a–f gray lines are the empirical exponential fits of reactivity as a function of the daily maximum temperature. In panels g–h the gray lines are the average reactivity. Linear fits to these data give slopes that are not meaningfully different than zero. The  $\text{C}_1$ – $\text{C}_2$  aldehydes are  $\text{H}_2\text{CO}$  and acetaldehyde (acetaldehyde's concentration was estimated, not measured; see below). The  $\text{C}_1$ – $\text{C}_3$  alcohols are methanol, ethanol, and isopropanol. Key molecules in the known-biogenic grouping are isoprene, methacrolein, MVK, glyoxal, limonene, and  $\alpha$ - and  $\beta$ -pinene.  $\text{C}_1$ – $\text{C}_3$  organic acids are formic acid, acetic acid, and propionic acid. All alkanes (panels e and h), alkenes, aromatics, and carbonyls, along with all other species included in Fig. 1 and Fig. A1 are listed in Table A2. Table A2 includes each compound's mean reactivity at low, moderate, and high daily maximum temperatures. If a temperature dependent OH rate expression is available we use the time varying temperature over the same time interval, not the daily maximum temperature. If no rate constant is available one is assigned by analogy to a compound with similar molecular structure, indicated with a double asterisk and an explanatory note. In order to sum the reactivities of many species, null daily average concentrations were filled using the temperature-dependent fit or average value as dictated by the observed temperature relationship. Methyl ethyl ketone is included in the temperature-dependent alkane  $\sum_i \text{VOCR}_i$ , as it exhibits clear temperature dependence; this was done so as to avoid introducing another temperature-dependent grouping. In a handful of instances, individual daily average  $\text{VOCR}_i$  outliers were removed prior to computing the temperature-dependent fit or mean.

The mixing ratio of acetaldehyde is estimated assuming (a) acyl peroxy nitrate products and aldehyde sources are co-located, i.e. that PPN:propanal is equal to



**Temperature  
dependent impacts of  
emission controls**

S. E. Pusede et al.

Title Page

Abstract

Introduction

Conclusions

References

Tables

Figures

◀

▶

◀

▶

Back

Close

Full Screen / Esc

Printer-friendly Version

Interactive Discussion



PAN:acetaldehyde, and (b) that acetaldehyde is the only PAN source molecule; methacrolein, biacetyl, MVK, and methyl glyoxal are also known PAN sources. Biacetyl, MVK, and methyl glyoxal were not measured during CalNex-SJV, so to test this second assumption, we approximated their concentrations via ratios to methacrolein, as observed during the Biosphere Effects on ARosol and Photochemistry Experiment (BEARPEX) (Lafranchi et al., 2009), which took place 15 June–31 July 2007 at a site located ~ 3 h downwind from an isoprene source region. Using the calculated acetaldehyde (Fig. A1 panel a), approximated biacetyl, MVK, and methyl glyoxal, and the measured methacrolein we find acetaldehyde to be ~ 80 % of the PAN source (compared to < 40 % at 30 °C at the BEARPEX site). The dominance of acetaldehyde to PAN formation is not unexpected in the southern SVJ given the low  $\text{VOCR}_{\text{isoprene}}$  and  $\text{VOCR}_{\text{macrolein}}$ . Alternatively, acetaldehyde can be calculated assuming steady state relationships with PAN,  $\text{HO}_2$ ,  $\text{RO}_2$ , NO, and  $\text{NO}_2$ . We find this approach yields an estimated  $\text{VOCR}_{\text{acetaldehyde}}$  that is ~ 3 times greater than the one we use in this analysis but with the same temperature dependence as we report. The larger acetaldehyde value would reduce the inferred missing  $\text{VOCR}$  by ~ 20 % but would not affect any other conclusion in this analysis.

MVK is estimated as 3 times the methacrolein concentration. This is the same ratio of MVK to methacrolein observed during BEARPEX-2007 (LaFranchi et al., 2009). We do not include an estimate for second-generation isoprene oxidation products. Due to the low levels of isoprene and methacrolein we expect second-generation oxidation product concentrations to also be small.

Ethane and benzene were estimated via observed relationships with propane and toluene, respectively, using the PAMS data record (Appendix B).



## Appendix B

### EPA PAMS dataset

The US Environmental Protection Agency (EPA) Photochemical Assessment Monitoring Stations (PAMS) network (<http://www.epa.gov/ttnamti1/pamsmain.html>) monitors a variety of organic molecules heavily weighted toward anthropogenic, unfunctionalized hydrocarbons emitted from light-duty vehicles. VOC samples are collected  $\sim 4$  times  $\text{day}^{-1}$  during the summer at 3 stations in the southern SJV: Shafter ( $35.504^\circ \text{N}$ ,  $119.272^\circ \text{W}$ ), Golden Street Avenue ( $35.386^\circ \text{N}$ ,  $119.015^\circ \text{W}$ ), and Arvin Bear Mountain Boulevard ( $35.208^\circ \text{N}$ ,  $118.784^\circ \text{W}$ ). We use the median of all data in a given year collected within the time interval of 1 a.m.–5 p.m. LT, as a result we may include, 1, or 2 data points from 1, 2, or 3 sites  $\text{day}^{-1}$ . We chose toluene to represent the trend in the temperature-independent  $\sum_i \text{VOCR}_i$ , as (a) it's daily average reactivity during CalNex-SJV was temperature-independent and (b) it was well sampled by the PAMS network 2001–2009. We compute the rate of decrease of  $\text{VOCR}_{\text{toluene}}$  to be  $\sim 6\% \text{yr}^{-1}$  over this time period.

We use the PAMS 2010 benzene:toluene and ethane:propane (10 a.m.–5 p.m. LT) to scale the CalNex-SJV observations of toluene and propane for  $\text{VOCR}_{\text{benzene}}$  and  $\text{VOCR}_{\text{ethane}}$ .

## Appendix C

### Impacts on $PO_3$ from future changes in $PHO_x$ and $NO/NO_x$

In Fig. 7 we tested three primary (direct) emissions control scenarios. Future changes in  $PHO_x$  and  $NO/NO_x$  will also impact  $PO_3$ , which we did not include in our three scenarios. Feedback effects result in changes to these parameters but have little effect on our conclusions. In Fig. C1 we separately test the temperature effects of  $\text{VOCR}$ ,  $PHO_x$ ,

### Temperature dependent impacts of emission controls

S. E. Pusede et al.

Title Page

Abstract

Introduction

Conclusions

References

Tables

Figures

⏪

⏩

◀

▶

Back

Close

Full Screen / Esc

Printer-friendly Version

Interactive Discussion



and  $\text{NO}/\text{NO}_x$  on  $\text{PO}_3$ . In each panel,  $\text{PO}_3$  is computed both with all parameters varying with temperature (at weekday  $\text{NO}_x$ ) (black) and with constant high-temperature average ( $34.6^\circ\text{C}$ ) values (the rate coefficients do vary with temperature) (gray). We test the temperature-dependent variables separately: VOCR (panel a),  $\text{PHO}_x$  (panel b), and  $\text{NO}/\text{NO}_x$  (panel c). First, decreases in  $\text{O}_3$  decrease  $\text{PHO}_x$  and increase  $\text{NO}/\text{NO}_x$ . For example, allowing  $\text{O}_3$  to be 50 % the  $\text{HO}_x$  source, a 20 % reduction in  $\text{O}_3$  effects an approximately 10 % decrease in  $\text{PHO}_x$ . This same decrease in  $\text{O}_3$  increases  $\text{NO}/\text{NO}_x$  by 25 % (at 80 ppb  $\text{O}_3$ , 5 ppb  $\text{NO}_2$ , 300 K, and  $j_{\text{NO}_2} = 0.009 \text{ s}^{-1}$ ). The two effects are near equal in magnitude and opposite in sign. Second, VOC emissions reductions work to decrease  $\text{PHO}_x$ , as  $\text{H}_2\text{CO}$  is, at some point, an oxidation product of nearly every organic molecule.  $\text{H}_2\text{CO}$  is  $\sim 25\%$  of  $\text{PHO}_x$  (during CalNex-SJV). If  $\text{H}_2\text{CO}$  decreases over the next decade according to Fig. 3, then a 15 % decrease (the upper bound) in  $\text{H}_2\text{CO}$  at high temperatures decreases  $\text{PHO}_x$  by less than 5 %, also at high temperatures, an effect too small to alter our conclusions.

*Acknowledgements.* This work was funded by the California Air Resources Board (contract CARB 08-316) and by the National Aeronautics and Space Administration (grant NNX10AR36G). We are grateful to John Karlik, Rick Ramirez, and the entire University of California Kern County Extension for logistical support during the CalNex-SJV project. We thank David Parrish for useful comments on our manuscript. We acknowledge the California Air Resources Board and the San Joaquin Valley Unified Air Pollution Control District for the temperature and  $\text{O}_3$  data. The findings and discussions described in this paper are those of the authors and do not necessarily represent the views of our sponsors.

## References

- Alanis, P., Ashkan, S., Krauter, C., Campbell, S., and Hasson, A. S.: Emissions of volatile fatty acids from feed at dairy facilities, *Atmos. Environ.*, 44, 5084–5092, doi:10.1016/j.atmosenv.2010.09.017, 2010.
- Atkinson, R.: Gas-phase tropospheric chemistry of organic compounds, *J. Phys. Chem. Ref. Data*, Monograph 2, 1–216, 1994.

## Temperature dependent impacts of emission controls

S. E. Pusede et al.

Title Page

Abstract

Introduction

Conclusions

References

Tables

Figures

◀

▶

◀

▶

Back

Close

Full Screen / Esc

Printer-friendly Version

Interactive Discussion



**Temperature  
dependent impacts of  
emission controls**

S. E. Pusede et al.

Title Page

Abstract

Introduction

Conclusions

References

Tables

Figures

◀

▶

◀

▶

Back

Close

Full Screen / Esc

Printer-friendly Version

Interactive Discussion



- Atkinson, R. and Arey, J.: Atmospheric degradation of volatile organic compounds, *Chem. Rev.*, 103, 4605–4638, doi:10.1021/cr0206420, 2003.
- Atkinson, R., Baulch, D. L., Cox, R. A., Hampson, R. F., Kerr, J. A., and Troe, J.: Evaluated kinetic and photochemical data for atmospheric chemistry supplement-IV – IUPAC subcommittee on gas kinetic data evaluation for atmospheric chemistry, *J. Phys. Chem. Ref. Data*, 21, 1125–1568, 1992.
- Atkinson, R., Baulch, D. L., Cox, R. A., Crowley, J. N., Hampson, R. F. Jr., Kerr, J. A., Rossi, M. J., and Troe, J., in: Summary of evaluated kinetic and photochemical data for atmospheric chemistry, edited by: Carver, G. D. and Cox, R. A., IUPAC Subcommittee on Gas Kinetic Evaluation for Atmospheric Chemistry, University of Cambridge, Cambridge, 1–56, 2001.
- Atkinson, R., Baulch, D. L., Cox, R. A., Crowley, J. N., Hampson, R. F., Hynes, R. G., Jenkin, M. E., Rossi, M. J., Troe, J., and IUPAC Subcommittee: Evaluated kinetic and photochemical data for atmospheric chemistry: Volume II – gas phase reactions of organic species, *Atmos. Chem. Phys.*, 6, 3625–4055, doi:10.5194/acp-6-3625-2006, 2006.
- Bishop, G. A. and Stedman, D. H.: A decade of on-road emissions measurements, *Environ. Sci. Technol.*, 42, 1651–1656, doi:10.1021/es702413b, 2008.
- Calvert, J. G., Atkinson, R., Becker, K. H., Kamens, R. M., Seinfeld, J. H., Wallington, T. J., and Yarwood, G.: The mechanism of atmospheric oxidation of aromatic hydrocarbons, Oxford University Press, New York, NY, 95, 2002.
- Cox, P., Delao, A., Komorniczak, A., and Weller, R.: The California Almanac of Emissions and Air Quality, California Air Resources Board, Sacramento, CA, 2009.
- Crouse, J. D., McKinney, K. A., Kwan, A. J., and Wennberg, P. O.: Measurement of gas-phase hydroperoxides by chemical ionization mass spectrometry, *Anal. Chem.*, 78, 6726–6732, doi:10.1021/ac0604235, 2006.
- Day, D. A., Wooldridge, P. J., Dillon, M. B., Thornton, J. A., and Cohen, R. C.: A thermal dissociation laser-induced fluorescence instrument for in situ detection of NO<sub>2</sub>, peroxy nitrates, alkyl nitrates, and HNO<sub>3</sub>, *J. Geophys. Res.-Atmos.*, 107, 4046, doi:10.1029/2001JD000779, 2002.
- de Gouw, J. A., Gilman, J. B., Borbon, A., Warneke, C., Kuster, W. C., Goldan, P. D. Holloway, J. S., Peischl, J., Ryerson, T. B., Parrish, D. D., Gentner, D. R., Goldstein, A. H., and Harley, R. A.: Increasing atmospheric burden of ethanol in the United States, *Geophys. Res. Lett.*, 39, L15803, doi:10.1029/2012GL052109, 2012.

**Temperature  
dependent impacts of  
emission controls**

S. E. Pusede et al.

Title Page

Abstract

Introduction

Conclusions

References

Tables

Figures

◀

▶

◀

▶

Back

Close

Full Screen / Esc

Printer-friendly Version

Interactive Discussion



Di Carlo, P., Brune, W. H., Martinez, M., Harder, H., Lesher, R., Ren, X. R., Thornberry, T., Carroll, M. A., Young, V., Shepson, P. B., Riemer, D., Apel, E., and Campbell, C.: Missing OH reactivity in a forest: evidence for unknown reactive biogenic VOCs, *Science*, 304, 722–725, doi:10.1126/science.1094392, 2004.

DiGangi, J. P., Boyle, E. S., Karl, T., Harley, P., Turnipseed, A., Kim, S., Cantrell, C., Maudlin III, R. L., Zheng, W., Flocke, F., Hall, S. R., Ullmann, K., Nakashima, Y., Paul, J. B., Wolfe, G. M., Desai, A. R., Kajii, Y., Guenther, A., and Keutsch, F. N.: First direct measurements of formaldehyde flux via eddy covariance: implications for missing in-canopy formaldehyde sources, *Atmos. Chem. Phys.*, 11, 10565–10578, doi:10.5194/acp-11-10565-2011, 2011.

Dillon, T. J., Holscher, D., Sivakumaran, V., Horowitz, A., and Crowley, J. N.: Kinetics of the reactions of HO with methanol (210–351 K) and with ethanol (216–368 K), *Phys. Chem. Chem. Phys.*, 7, 349–355, doi:10.1039/b413961e, 2005.

Fares, S., Gentner, D. R., Park, J.-H., Ormeño, E., Karlik, J., and Goldstein, A. H.: Biogenic emissions from Citrus species in California, *Atmos. Environ.*, 45, 4557–4568, doi:10.1016/j.atmosenv.2011.05.066, 2011.

Fares, S., Park, J.-H., Gentner, D. R., Weber, R., Ormeño, E., Karlik, J., and Goldstein, A. H.: Seasonal cycles of biogenic volatile organic compound fluxes and concentrations in a California citrus orchard, *Atmos. Chem. Phys.*, 12, 9865–9880, doi:10.5194/acp-12-9865-2012, 2012.

Farmer, D. K., Perring, A. E., Wooldridge, P. J., Blake, D. R., Baker, A., Meinardi, S., Huey, L. G., Tanner, D., Vargas, O., and Cohen, R. C.: Impact of organic nitrates on urban ozone production, *Atmos. Chem. Phys.*, 11, 4085–4094, doi:10.5194/acp-11-4085-2011, 2011.

Galbally, I. E. and Kirstine, W.: The production of methanol by flowering plants and the global cycle of methanol, *J. Atmos. Chem.*, 43, 195–229, doi:10.1023/A:1020684815474, 2002.

Gentner, D. R., Harley, R. A., Miller, A. M., and Goldstein, A. H.: Diurnal and seasonal variability of gasoline-related volatile organic compound emissions in Riverside, California, *Environ. Sci. Technol.*, 43, 4247–4252, doi:10.1021/es9006228, 2009.

Gentner, D. R., Isaacman, G., Worton, D. R., Chan, A. W. H., Dallmann, T. R., Davis, L., Liu, S., Day, D. A., Russell, L. M., Wilson, K. R., Weber, R., Guha, A., Harley, R. A., and Goldstein, A. H.: Elucidating secondary organic aerosol from diesel and gasoline vehicles through detailed characterization of organic carbon emissions, *P. Natl. Acad. Sci.*, 45, 18318–18323, doi:10.1073/pnas.1212272109, 2012.

**Temperature  
dependent impacts of  
emission controls**

S. E. Pusede et al.

Title Page

Abstract

Introduction

Conclusions

References

Tables

Figures

◀

▶

◀

▶

Back

Close

Full Screen / Esc

Printer-friendly Version

Interactive Discussion

Gentner, D. R., Ford, T. B., Guha, A., Boulanger, K., Brioude, J., Angevine, W. M., de Gouw, J. A., Warneke, C., Gilman, J. B., Ryerson, T. B., Peischl, J., Meinardi, S., Blake, D. R., Atlas, E., Lonneman, W. A., Kleindienst, T. E., Beaver, M. R., St. Clair, J. M., Wennberg, P. O., Vandenberg, T. C., Markovic, M. Z., Murphy, J. G., Harley, R. A., and Goldstein, A. H.: Emissions of organic carbon and methane from petroleum and dairy operations in California's San Joaquin Valley, in preparation, 2013a.

Gentner, D. R., Ormeño, E., Fares, S., Ford, T. B., Weber, R., Park, J.-H., Brioude, J., Angevine, W. M., Karlik, J. F., and Goldstein, A. H.: Emissions of biogenic gas-phase organic carbon from agricultural crops and their potential implications of air quality, in preparation, 2013b.

Guenther, A. B., Zimmerman, P. R., Harley, P. C., Monson, R. K., and Fall, R.: Isoprene and monoterpene emission rate variability: model evaluations and sensitivity analyses, *J. Geophys. Res.*, 98, 12609–12617, doi:10.1029/93JD00527, 1993.

Harley, R. A., Hooper, D. S., Kean, A. J., Kirchstetter, T. W., Hesson, J. M., Balberan, N. T., Stevenson, E. D., and Kendall, G. R.: Effects of reformulated gasoline and motor vehicle fleet turnover on emissions and ambient concentrations of benzene, *Environ. Sci. Technol.*, 40, 5084–5088, doi:10.1021/es0604820, 2006.

Hottel, J. R., Huisman, A. J., Digangi, J. P., Kammrath, A., Galloway, M. M., Coens, K. L., and Keutsch, F. N.: A laser induced fluorescence-based instrument for in-situ measurements of atmospheric formaldehyde, *Environ. Sci. Technol.*, 43, 790–795, doi:10.1021/es801621f, 2009.

Howard, C. J., Kumar, A., Malkina, I., Mitloehner, F., Green, P. G., Flocchini, R. G., and Kleeman, M. J.: Reactive organic gas emissions from livestock feed contribute significantly to ozone production in Central California, *Environ. Sci. Technol.*, 44, 2309–2314, doi:10.1021/es902864u, 2010a.

Howard, C. J., Kumar, A., Mitloehner, F., Stackhouse, K., Green, P. G., Flocchini, R. G., and Kleeman, M. J.: Direct measurements of the ozone formation potential from livestock and poultry waste emissions, *Environ. Sci. Technol.*, 44, 2292–2298, doi:10.1021/es901916b, 2010b.

Hu, J. L., Howard, C. J., Mitloehner, F., Green, P. G., and Kleeman, M. J.: Mobile source and livestock feed contributions to regional ozone formation in Central California, *Environ. Sci. Technol.*, 46, 2781–2789, doi:10.1021/es203369p, 2012.

**Temperature  
dependent impacts of  
emission controls**

S. E. Pusede et al.

Title Page

Abstract

Introduction

Conclusions

References

Tables

Figures

◀

▶

◀

▶

Back

Close

Full Screen / Esc

Printer-friendly Version

Interactive Discussion



Huisman, A. J., Hottle, J. R., Coens, K. L., DiGangi, J. P., Galloway, M. M., Kammrath, A., and Keutsch, F. N.: Laser-induced phosphorescence for the in situ detection of glyoxal at part per trillion mixing ratios, *Anal. Chem.*, 80, 5884–5891, doi:10.1021/ac800407b, 2008.

Huisman, A. J., Hottle, J. R., Galloway, M. M., DiGangi, J. P., Coens, K. L., Choi, W., Faloon, I. C., Gilman, J. B., Kuster, W. C., de Gouw, J., Bouvier-Brown, N. C., Goldstein, A. H., LaFranchi, B. W., Cohen, R. C., Wolfe, G. M., Thornton, J. A., Docherty, K. S., Farmer, D. K., Cubison, M. J., Jimenez, J. L., Mao, J., Brune, W. H., and Keutsch, F. N.: Photochemical modeling of glyoxal at a rural site: observations and analysis from BEARPEX 2007, *Atmos. Chem. Phys.*, 11, 8883–8897, doi:10.5194/acp-11-8883-2011, 2011.

Karl, T., Guenther, A., Lindinger, C., Jordan, A., Fall, R., and Lindinger, W.: Eddy covariance measurements of oxygenated volatile organic compound fluxes from crop harvesting using a redesigned proton-transfer-reaction mass spectrometer, *J. Geophys. Res.-Atmos.*, 106, 24157–24167, doi:10.1029/2000JD000112, 2001.

Kirchstetter, T. W., Singer, B. C., Harley, R. A., Kendall, G. R., and Hesson, J. M.: Impact of California reformulated gasoline on motor vehicle emissions. 2. Volatile organic compound speciation and reactivity, *Environ. Sci. Technol.*, 33, 329–336, doi:10.1021/es980374g, 1999a.

Kirchstetter, T. W., Singer, B. C., Harley, R. A., Kendall, G. R., and Traverse, M.: Impact of California reformulated gasoline on motor vehicle emissions, 1. Mass emission rates, *Environ. Sci. Technol.*, 33, 318–328, doi:10.1021/es9803714, 1999b.

Kovacs, T. A. and Brune, W. H.: Total OH loss rate measurement, *J. Atmos. Chem.*, 39, 105–122, doi:10.1023/A:1010614113786, 2001.

Kovacs, T. A., Brune, W. H., Harder, H., Martinez, M., Simpas, J. B., Frost, G. J., Williams, E., Jobson, T., Stroud, C., Young, V., Fried, A., and Wert, B.: Direct measurements of urban OH reactivity during Nashville SOS in summer 1999, *J. Environ. Monitor.*, 5, 68–74, doi:10.1039/b204339d, 2003.

LaFranchi, B. W., Wolfe, G. M., Thornton, J. A., Harrold, S. A., Browne, E. C., Min, K. E., Wooldridge, P. J., Gilman, J. B., Kuster, W. C., Goldan, P. D., de Gouw, J. A., McKay, M., Goldstein, A. H., Ren, X., Mao, J., and Cohen, R. C.: Closing the peroxy acetyl nitrate budget: observations of acyl peroxy nitrates (PAN, PPN, and MPAN) during BEARPEX 2007, *Atmos. Chem. Phys.*, 9, 7623–7641, doi:10.5194/acp-9-7623-2009, 2009.

LaFranchi, B. W., Goldstein, A. H., and Cohen, R. C.: Observations of the temperature dependent response of ozone to NO<sub>x</sub> reductions in the Sacramento, CA urban plume, *Atmos. Chem. Phys.*, 11, 6945–6960, doi:10.5194/acp-11-6945-2011, 2011.

**Temperature  
dependent impacts of  
emission controls**

S. E. Pusede et al.

Title Page

Abstract

Introduction

Conclusions

References

Tables

Figures

◀

▶

◀

▶

Back

Close

Full Screen / Esc

Printer-friendly Version

Interactive Discussion



- Lou, S., Holland, F., Rohrer, F., Lu, K., Bohn, B., Brauers, T., Chang, C.C., Fuchs, H., Häsel, R., Kita, K., Kondo, Y., Li, X., Shao, M., Zeng, L., Wahner, A., Zhang, Y., Wang, W., and Hofzumahaus, A.: Atmospheric OH reactivities in the Pearl River Delta – China in summer 2006: measurement and model results, *Atmos. Chem. Phys.*, 10, 11243–11260, doi:10.5194/acp-10-11243-2010, 2010.
- Madronich, S.: Photodissociation in the atmosphere. 1. Actinic flux and the effects of ground reflections and clouds, *J. Geophys. Res.-Atmos.*, 92, 9740–9752, doi:10.1029/JD092iD08p09740, 1987.
- Malkina, I. L., Kumar, A., Green, P. G., and Mitloehner, F. M.: Identification and quantitation of volatile organic compounds emitted from dairy silages and other feedstuffs, *J. Environ. Qual.*, 40, 28–36, doi:10.2134/jeq2010.0302, 2011.
- Mao, J., Ren, X., Zhang, L., Van Duin, D. M., Cohen, R. C., Park, J.-H., Goldstein, A. H., Paulot, F., Beaver, M. R., Crounse, J. D., Wennberg, P. O., DiGangi, J. P., Henry, S. B., Keutsch, F. N., Park, C., Schade, G. W., Wolfe, G. M., Thornton, J. A., and Brune, W. H.: Insights into hydroxyl measurements and atmospheric oxidation in a California forest, *Atmos. Chem. Phys.*, 12, 8009–8020, doi:10.5194/acp-12-8009-2012, 2012.
- Markovic, M. Z., VandenBoer, T. C., and Murphy, J. G.: Characterization and optimization of an online system for the simultaneous measurement of atmospheric water-soluble constituents in the gas and particle phases, *J. Environ. Monit.*, 14, 1872–1884, doi:10.1039/c2em00004k, 2012.
- McDonald, B. C., Dallmann, T. R., Martin, E. W., and Harley, R. A.: Long-term trends in nitrogen oxide emissions from motor vehicles at national, state, and air basin scales, *J. Geophys. Res.-Atmos.*, 117, D00V18, doi:10.1029/2012JD018304, 2012.
- Mielke, L. H., Furgeson, A., and Osthoff, H. D.: Observation of ClNO<sub>2</sub> in a mid-continental urban environment, *Environ. Sci. Technol.*, 45, 8889–8896, doi:10.1021/es201955u, 2011.
- Min, K.-E., Pusede, S. E., Browne, E. C., LaFranchi, B. W., Wooldridge, P. J., and Cohen, R. C.: Eddy covariance fluxes and vertical concentration gradient measurements of NO and NO<sub>2</sub> over a ponderosa pine ecosystem: observational evidence for within canopy removal of NO<sub>x</sub>, *Atmos. Chem. Phys. Discuss.*, 13, 12437–12484, doi:10.5194/acpd-13-12437-2013, 2013.
- Murphy, J. G., Day, D. A., Cleary, P. A., Wooldridge, P. J., Millet, D. B., Goldstein, A. H., and Cohen, R. C.: The weekend effect within and downwind of Sacramento – Part 1: Observations of ozone, nitrogen oxides, and VOC reactivity, *Atmos. Chem. Phys.*, 7, 5327–5339, doi:10.5194/acp-7-5327-2007, 2007.



**Temperature  
dependent impacts of  
emission controls**

S. E. Pusede et al.

Title Page

Abstract

Introduction

Conclusions

References

Tables

Figures

◀

▶

◀

▶

Back

Close

Full Screen / Esc

Printer-friendly Version

Interactive Discussion



Ormeño, E., Gentner, D. R., Fares, S., Karlik, J., Park, J. H., and Goldstein, A. H.: Sesquiterpenoid emissions from agricultural crops: correlations to monoterpene emissions and leaf terpene content, *Environ. Sci. Technol.*, 44, 3758–3764, doi:10.1021/es903674m, 2010.

Osthoff, H. D., Roberts, J. M., Ravishankara, A. R., Williams, E. J., Lerner, B. M., Sommariva, R., Bates, T. S., Coffman, D., Quinn, P. K., Dibb, J. E., Stark, H., Burkholder, J. B., Talukdar, R. K., Meagher, J., Fehsenfeld, F. C., and Brown, S. S.: High levels of nitryl chloride in the polluted subtropical marine boundary layer, *Nat. Geosci.*, 1, 324–328, doi:10.1038/ngeo177, 2008.

Park, J.-H., Goldstein, A. H., Timkovsky, J., Fares, S., Weber, R., Karlik, J., and Holzinger, R.: Eddy covariance emission and deposition flux measurements using proton transfer reaction – time of flight – mass spectrometry (PTR-TOF-MS): comparison with PTR-MS measured vertical gradients and fluxes, *Atmos. Chem. Phys.*, 13, 1439–1456, doi:10.5194/acp-13-1439-2013, 2013.

Parrish, D. D.: Critical evaluation of US on-road vehicle emission inventories, *Atmos. Environ.*, 40, 2288–2300, doi:10.1016/j.atmosenv.2005.11.033, 2006.

Parrish, D. D., Trainer, M., Hereid, D., Williams, E. J., Olszyna, K. J., Harley, R. A., Meagher, J. F., and Fehsenfeld, F. C.: Decadal change in carbon monoxide to nitrogen oxide ratio in US vehicular emissions, *J. Geophys. Res.-Atmos.*, 107, 4140, doi:10.1029/2001JC000720, 2002.

Perring, A. E., Pusede, S. E., and Cohen, R. C.: An observational perspective on the atmospheric impacts of alkyl and multifunctional nitrates on ozone and secondary organic aerosol, *Chem. Rev.*, 113, 5848–5870, doi:10.1021/cr300520x, 2013.

Pierson, W. R., Schorran, D. E., Fujita, E. M., Sagebiel, J. C., Lawson, D. R., and Tanner, R. L.: Assessment of nontailpipe hydrocarbon emissions from motor vehicles, *J. Air Waste Manage. Assoc.*, 49, 498–519, 1999.

Pusede, S. E. and Cohen, R. C.: On the observed response of ozone to NO<sub>x</sub> and VOC reactivity reductions in San Joaquin Valley California 1995–present, *Atmos. Chem. Phys.*, 12, 8323–8339, doi:10.5194/acp-12-8323-2012, 2012.

Ren, X., Sanders, J. E., Rajendran, A., Weber, R. J., Goldstein, A. H., Pusede, S. E., Browne, E. C., Min, K.-E., and Cohen, R. C.: A relaxed eddy accumulation system for measuring vertical fluxes of nitrous acid, *Atmos. Meas. Tech.*, 4, 2093–2103, doi:10.5194/amt-4-2093-2011, 2011.



**Temperature  
dependent impacts of  
emission controls**

S. E. Pusede et al.

Title Page

Abstract

Introduction

Conclusions

References

Tables

Figures

◀

▶

◀

▶

Back

Close

Full Screen / Esc

Printer-friendly Version

Interactive Discussion

Russell, A. R., Valin, L. C., and Cohen, R. C.: Trends in OMI NO<sub>2</sub> observations over the United States: effects of emission control technology and the economic recession, *Atmos. Chem. Phys.*, 12, 12197–12209, doi:10.5194/acp-12-12197-2012, 2012.

Rubin, J. I., Kean, A. J., Harley, R. A., Millet, D. B., and Goldstein, A. H.: Temperature dependence of volatile organic compound evaporative emissions from motor vehicles, *J. Geophys. Res.-Atmos.*, 111, D03305, doi:10.1029/2005JD006458, 2006.

Ryerson, T. B., Andrews, A. E., Angevine, W. M., Bates, T. S., Brock, C. A., Cairns, B., Cohen, R. C., Cooper, O. R., de Gouw, J. A., Fehsenfeld, F. C., Ferrare, R. A., Fischer, M. L., Flagan, R. C., Goldstein, A. H., Hair, J. W., Hardesty, R. M., Hostetler, C. A., Jimenez, J. L., Langford, A. O., McCauley, E., McKeen, S. A., Molina, L. T., Nenes, A., Oltmans, S. J., Parrish, D. D., Pederson, J. R., Pierce, R. B., Prather, K., Quinn, P. K., Seinfeld, J. H., Senff, C. J., Sorooshian, A., Stutz, J., Surratt, J. D., Trainer, M., Volkamer, R., Williams, E. J., and Wofsy, S. C.: The 2010 California Research at the Nexus of Air Quality and Climate Change (CalNex) field study, *J. Geophys. Res.-Atmos.*, 118, 5830–5866, doi:10.1002/jgrd.50331, 2013.

Sander, S. P., Friedl, R. R., Golden, D. M., Kurylo, M. J., Huie, R. E., Orkin, V. L., Moortgat, G. K., Ravishankara, A. R., Kolb, C. E., Molina, M. J., and Finlayson-Pitts, B. J.: Chemical kinetics and photochemical data for use in atmospheric studies, Evaluation No. 14, JPL Publication 02-25, Jet Propulsion Laboratory, Pasadena, available at: [http://jpldataeval.jpl.nasa.gov/pdf/JPL\\_02-25\\_rev02.pdf](http://jpldataeval.jpl.nasa.gov/pdf/JPL_02-25_rev02.pdf) (last access: 1 October 2011), 2003.

Schade, G. W. and Goldstein, A. H.: Fluxes of oxygenated volatile organic compounds from a ponderosa pine plantation, *J. Geophys. Res.-Atmos.*, 106, 3111–3123, doi:10.1029/2000JD900592, 2001.

Shaw, S. L., Mitloehner, F. M., Jackson, W., Depeters, E. J., Fadel, J. G., Robinson, P. H., Holzinger, R., and Goldstein, A. H.: Volatile organic compound emissions from dairy cows and their waste as measured by proton-transfer-reaction mass spectrometry, *Environ. Sci. Technol.*, 41, 1310–1316, doi:10.1021/es061475e, 2007.

Sprengnether, M. M., Demerjian, K. L., Dransfield, T. J., Clarke, J. S., Anderson, J. G., and Donahue, N. M.: Rate constants of nine C<sub>6</sub>–C<sub>9</sub> alkanes with OH from 230 to 379 K: chemical tracers for OH, *J. Phys. Chem. A*, 113, 5030–5038, doi:10.1021/jp810412m, 2009.

Steiner, A. L., Cohen, R. C., Harley, R. A., Tonse, S., Millet, D. B., Schade, G. W., and Goldstein, A. H.: VOC reactivity in central California: comparing an air quality model to

ground-based measurements, *Atmos. Chem. Phys.*, 8, 351–368, doi:10.5194/acp-8-351-2008, 2008.

Thornton, J. A., Wooldridge, P. J., and Cohen, R. C.: Atmospheric NO<sub>2</sub>: In situ laser-induced fluorescence detection at parts per trillion mixing ratios, *Anal. Chem.*, 72, 528–539, doi:10.1021/ac9908905, 2000.

Thornton, J. A., Kercher, J. P., Riedel, T. P., Wagner, N. L., Cozic, J., Holloway, J. S., Dube, W. P., Wolfe, G. M., Quinn, P. K., Middlebrook, A. M., Alexander, B., and Brown, S. S.: A large atomic chlorine source inferred from mid-continental reactive nitrogen chemistry, *Nature*, 464, 271–274, doi:10.1038/nature08905, 2010.

VandenBoer, T. C., Markovic, M. Z., Sanders, J. E., Ren, X., Pusede, S. E., Rollins, A. W., Browne, E. C., Cohen, R. C., Weber, R. J., Goldstein, A. H., Brune, W. H., and Murphy, J. G.: Evidence for a nitrous acid (HONO) reservoir at the ground surface in Bakersfield, CA during CalNex 2010, *J. Geophys. Res.*, submitted, 2013.

Veefkind, J. P., de Haan, J. F., Brinksma, E. J., Kroon, M., and Levelt, P. F.: Total ozone from the Ozone Monitoring Instrument (OMI) using the DOAS technique, *IEEE Trans. Geo. Rem. Sens.*, 44, 5, 1239–1244, doi:10.1109/TGRS.2006.871204, 2006.

Wolfe, G. M., Thornton, J. A., Yatavelli, R. L. N., McKay, M., Goldstein, A. H., LaFranchi, B., Min, K.-E., and Cohen, R. C.: Eddy covariance fluxes of acyl peroxy nitrates (PAN, PPN and MPAN) above a Ponderosa pine forest, *Atmos. Chem. Phys.*, 9, 615–634, doi:10.5194/acp-9-615-2009, 2009.

Yamada, T., Taylor, P. H., Goumri, A., and Marshall, P.: The reaction of OH with acetone and acetone-d(6) from 298 to 832 K: Rate coefficients and mechanism, *J. Chem. Phys.*, 119, 10600–10606, doi:10.1063/1.1619950, 2003.

Temperature  
dependent impacts of  
emission controls

S. E. Pusede et al.

Title Page

Abstract

Introduction

Conclusions

References

Tables

Figures

◀

▶

◀

▶

Back

Close

Full Screen / Esc

Printer-friendly Version

Interactive Discussion



## Temperature dependent impacts of emission controls

S. E. Pusede et al.

**Table 1.**  $PO_3$  (ppb h<sup>-1</sup>) computed with an analytical model parameterized with CalNex-SJV observations. Row 1:  $PO_3$  calculated at the 2010 average low (24.7 °C), moderate (30.8 °C), and high (36.4 °C) temperatures. Row 2: Number of violations of the 8 h California O<sub>3</sub> standard in Bakersfield in 2010 day<sup>-1</sup> by temperature and by weekday/weekend. Uncertainties are computed as counting errors as  $0.5(N)^{1/2}/N$ , where  $N$  is the total numbers of days in that temperature and day-of-week regime. Rows 3–5:  $PO_3$  (ppb h<sup>-1</sup>) calculated with 50 % lower NO<sub>x</sub>, with 50 % lower temperature-independent  $\sum_i VO_{CR}_i$ , and with both 50 % lower NO<sub>x</sub> and 50 % lower temperature-independent  $\sum_i VO_{CR}_i$ . Also shown are the percent differences (%) between the 2010 CalNex constrained  $PO_3$  and that computed with the emissions reduction.  $PO_3$  is rounded to the nearest ppb h<sup>-1</sup>. The relevant uncertainty is not in  $PO_3$  itself but in the derivative of  $PO_3$  with respect to NO<sub>x</sub>.

	Low (at 24.7 °C)		Moderate (at 30.8 °C)		High (at 36.4 °C)	
	Weekdays	Weekends	Weekdays	Weekends	Weekdays	Weekends
CalNex-SJV						
$PO_3$ (ppb h <sup>-1</sup> )	10	12	18	15	26	15
Bakersfield 2010						
Violations day <sup>-1</sup>	0 (±0.10)	0 (±0.17)	0.22 (±0.09)	0.25 (±0.11)	0.76 (±0.07)	0.43 (±0.10)
-50 % NO <sub>x</sub>						
$PO_3$ (ppb h <sup>-1</sup> )	12	8	16	9	17	8
Impact (%)	26	-31	-12	-42	-33	-48
-50 % temperature-independent $\sum_i VO_{CR}_i$						
$PO_3$ (ppb h <sup>-1</sup> )	7	11	16	14	25	15
Impact (%)	-26	-12	-10	-3	-4	-1
-50 % NO <sub>x</sub> and -50 % temperature-independent $\sum_i VO_{CR}_i$						
$PO_3$ (ppb h <sup>-1</sup> )	11	8	15	8	17	8
Impact (%)	7	-35	-15	-43	-33	-46

[Title Page](#)
[Abstract](#)
[Introduction](#)
[Conclusions](#)
[References](#)
[Tables](#)
[Figures](#)
[◀](#)
[▶](#)
[◀](#)
[▶](#)
[Back](#)
[Close](#)
[Full Screen / Esc](#)
[Printer-friendly Version](#)
[Interactive Discussion](#)


## Temperature dependent impacts of emission controls

S. E. Pusede et al.

Title Page

Abstract

Introduction

Conclusions

References

Tables

Figures

◀

▶

◀

▶

Back

Close

Full Screen / Esc

Printer-friendly Version

Interactive Discussion



**Table A1.** Species, measurement accuracy, analytical technique, and reference for each CalNex-SJV observation included in our analysis. Many species are measured with higher precision than accuracy. See original references for details. All CalNex data are accessible to the public at <http://www.esrl.noaa.gov/csd/groups/csd7/measurements/2010calnex/>.

Species	Accuracy ( $\pm$ %)	Analytical technique	Reference
VOCs	5	gas chromatography-mass spectrometer	Gentner et al. (2012)
CH <sub>2</sub> O	30	laser induced fluorescence (LIF)	Hottle et al. (2009); DiGangi et al. (2011)
PAN and PPN	21	chemical ionization mass spectrometry (CIMS)	Wolfe et al. (2009)
C <sub>1</sub> –C <sub>3</sub> acids	50	CIMS	Crounse et al. (2006)
glyoxal	20	laser induced phosphorescence	Huisman et al. (2008)
CO	0.5	infrared (IR) absorption	
CH <sub>4</sub>	1	IR absorption	
OH reactivity	32	OH decay by LIF	Kovacs et al. (2003)
NO <sub>2</sub>	5	LIF	Thornton et al. (2000)
NO	7	chemiluminescence	Min et al. (2013)
NH <sub>3</sub> , SO <sub>2</sub>	20, 15	ambient ion monitor-ion chromatography	Markovic et al. (2012)
HONO	15	long path absorption photometry	Ren et al. (2011)
HNO <sub>3</sub>	50	CIMS	Crounse et al. (2006)
$\Sigma$ ANs	15	thermal dissociation-LIF	Day et al. (2002)
O <sub>3</sub>	1 ppb	UV absorbance	Dasibi 1008PC O <sub>3</sub> monitor
H <sub>2</sub> O <sub>2</sub>	50	CIMS	Crounse et al. (2006)

Temperature  
dependent impacts of  
emission controls

S. E. Pusede et al.

Title Page

Abstract

Introduction

Conclusions

References

Tables

Figures

◀

▶

◀

▶

Back

Close

Full Screen / Esc

Printer-friendly Version

Interactive Discussion



**Table A2.** Mean  $\text{VOCR}_i$  of all species included in  $\sum_i \text{VOCR}_i$  with  $1\sigma$ , indicating the observed variability, over low ( $17\text{--}27^\circ\text{C}$ ), moderate ( $28\text{--}33^\circ\text{C}$ ), and high ( $34\text{--}45^\circ\text{C}$ ) daily maximum temperatures. Species are arranged by Fig. 1 grouping and listed greatest to smallest high-temperature  $\text{s}^{-1}$ . The  $\text{VOC}_i + \text{OH}$  rate constants or temperature-dependent rate expressions are also listed with associated references. The concentrations of the starred species, acetaldehyde, MVK, ethane, and benzene, were estimated (Appendix A). Double starred  $k_{\text{OH}}$  values were estimated by analogy to compounds with similar molecular structure and these include explanatory notes.

Species	Mean ( $\pm 1\sigma$ ) $\text{VOCR}$ ( $\text{s}^{-1}$ ) by temperature			$k$ or $k(T)$ ( $\text{cm}^3 \text{molecule}^{-1} \text{s}^{-1}$ )	Reference
	Low	Moderate	High		
$\text{C}_1\text{--}\text{C}_2$ aldehydes					
$\text{H}_2\text{CO}$	$4.4 (\pm 1.0) \times 10^{-1}$	$6.5 (\pm 0.5) \times 10^{-1}$	$7.9 (\pm 0.8) \times 10^{-1}$	$1.20 \times 10^{-14} \text{Texp}(287/T)$	(a)
acetaldehyde*	$2.3 (\pm 0.6) \times 10^{-1}$	$4.1 (\pm 1.0) \times 10^{-1}$	$6.2 (\pm 0.9) \times 10^{-1}$	$4.4 \times 10^{-12} \text{exp}(365/T)$	(a)
$\text{C}_1\text{--}\text{C}_3$ alcohols					
methanol	$1.6 (\pm 0.6) \times 10^{-1}$	$3.6 (\pm 0.6) \times 10^{-1}$	$5.5 (\pm 1.8) \times 10^{-1}$	$3.82 \times 10^{-19} \text{T}^{2.4} \text{exp}(300/T)$	(b)
ethanol	$3.4 (\pm 1.4) \times 10^{-1}$	$4.6 (\pm 1.4) \times 10^{-1}$	$4.6 (\pm 2.0) \times 10^{-1}$	$6.72 \times 10^{-18} \text{T}^2 \text{exp}(510/T)$	(b)
isopropanol	$8.9 (\pm 3.4) \times 10^{-3}$	$9.7 (\pm 3.3) \times 10^{-3}$	$1.2 (\pm 0.6) \times 10^{-2}$	$4.03 \times 10^{-18} \text{T}^2 \text{exp}(792/T)$	(a)
Known-biogenic VOCs					
isoprene	$9.0 (\pm 3.2) \times 10^{-2}$	$1.6 (\pm 0.4) \times 10^{-1}$	$2.4 (\pm 0.5) \times 10^{-1}$	$2.7 \times 10^{-11} \text{exp}(390/T)$	(a)
methacrolein	$6.2 (\pm 0.5) \times 10^{-2}$	$8.0 (\pm 1.8) \times 10^{-2}$	$1.2 (\pm 2.6) \times 10^{-1}$	$8.0 \times 10^{-12} \text{exp}(380/T)$	(a)
d-limonene	$2.9 (\pm 0.2) \times 10^{-2}$	$3.8 (\pm 0.9) \times 10^{-2}$	$5.7 (\pm 1.3) \times 10^{-2}$	$4.28 \times 10^{-11} \text{exp}(401/T)$	(a)
MVK*	$3.4 (\pm 1.7) \times 10^{-2}$	$3.7 (\pm 1.7) \times 10^{-2}$	$3.8 (\pm 2.0) \times 10^{-2}$	$2.6 \times 10^{-12} \text{exp}(610/T)$	(a)
glyoxal	$1.6 (\pm 0.4) \times 10^{-2}$	$2.6 (\pm 0.4) \times 10^{-2}$	$2.9 (\pm 0.7) \times 10^{-2}$	$1.10 \times 10^{-11}$	(a)
$\alpha$ -pinene	$2.0 (\pm 1.2) \times 10^{-2}$	$2.1 (\pm 1.1) \times 10^{-2}$	$2.4 (\pm 1.1) \times 10^{-2}$	$12.1 \times 10^{-12} \text{exp}(436/T)$	(a)
d $\beta$ -carene	$1.6 (\pm 1.0) \times 10^{-2}$	$2.1 (\pm 0.5) \times 10^{-2}$	$2.2 (\pm 0.5) \times 10^{-2}$	$8.8 \times 10^{-11}$	(a)
sabinene	$5.3 (\pm 3.8) \times 10^{-3}$	$7.3 (\pm 2.0) \times 10^{-3}$	$1.0 (\pm 0.2) \times 10^{-2}$	$1.17 \times 10^{-10}$	(a)
acetone	$1.5 (\pm 0.5) \times 10^{-3}$	$3.4 (\pm 1.1) \times 10^{-3}$	$5.8 (\pm 3.7) \times 10^{-3}$	$4.0 \times 10^{-24} \text{T}^4 \text{exp}(453/T)$	(c)
camphene	$2.8 (\pm 0.7) \times 10^{-3}$	$3.4 (\pm 1.0) \times 10^{-3}$	$3.9 (\pm 1.1) \times 10^{-3}$	$5.3 \times 10^{-11}$	(a)
$\beta$ -pinene	$2.2 (\pm 1.3) \times 10^{-3}$	$2.8 (\pm 0.6) \times 10^{-3}$	$3.4 (\pm 0.6) \times 10^{-3}$	$15.5 \times 10^{-12} \text{exp}(467/T)$	(a)
nopinone	$6.9 (\pm 2.3) \times 10^{-4}$	$6.3 (\pm 4.0) \times 10^{-4}$	$6.0 (\pm 2.4) \times 10^{-4}$	$1.5 \times 10^{-11}$	(a)
$\text{CH}_4$					
$\text{CH}_4$	$2.8 (\pm 0.2) \times 10^{-1}$	$8.9 (\pm 0.2) \times 10^{-1}$	$3.6 (\pm 0.2) \times 10^{-1}$	$1.85 \times 10^{-20} \text{T}^{2.85} \text{exp}(-987/T)$	(a)
Temperature-dependent alkanes					
isopentane	$3.7 (\pm 0.9) \times 10^{-2}$	$6.3 (\pm 1.8) \times 10^{-2}$	$7.2 (\pm 2.2) \times 10^{-2}$	$3.6 \times 10^{-12}$	(a)
propane	$5.0 (\pm 2.3) \times 10^{-2}$	$5.0 (\pm 1.8) \times 10^{-2}$	$5.9 (\pm 2.1) \times 10^{-2}$	$1.65 \times 10^{-17} \text{T}^2 \text{exp}(-87/T)$	(a)
<i>n</i> -butane	$3.3 (\pm 1.8) \times 10^{-2}$	$2.9 (\pm 1.6) \times 10^{-2}$	$3.6 (\pm 1.5) \times 10^{-2}$	$1.81 \times 10^{-17} \text{T}^2 \text{exp}(114/T)$	(a)
<i>n</i> -pentane	$2.0 (\pm 0.4) \times 10^{-2}$	$3.0 (\pm 0.9) \times 10^{-2}$	$3.3 (\pm 1.0) \times 10^{-2}$	$2.52 \times 10^{-17} \text{T}^2 \text{exp}(158/T)$	(a)

Table A2. Continued.

Species	Mean ( $\pm 1\sigma$ ) VOCR ( $s^{-1}$ ) by temperature			$k$ or $k(T)$ ( $cm^3 molecule^{-1} s^{-1}$ )	Reference
	Low	Moderate	High		
2-methylpentane and 2,3-dimethylbutane	$1.5 (\pm 0.3) \times 10^{-2}$	$2.3 (\pm 0.6) \times 10^{-2}$	$2.5 (\pm 0.8) \times 10^{-2}$	$5.2 \times 10^{-12}$	(a) <sup>1</sup>
methylcyclopentane	$1.2 (\pm 0.4) \times 10^{-2}$	$1.6 (\pm 0.6) \times 10^{-2}$	$1.7 (\pm 0.5) \times 10^{-2}$	$7.66 \times 10^{-12}$	(d)
<i>n</i> -hexane	$7.7 (\pm 2.2) \times 10^{-3}$	$1.0 (\pm 0.3) \times 10^{-2}$	$1.1 (\pm 0.3) \times 10^{-2}$	$2.54 \times 10^{-14} \text{Temp}(-112/T)$	(a)
3-methylpentane	$6.7 (\pm 1.7) \times 10^{-3}$	$9.8 (\pm 3.2) \times 10^{-3}$	$1.1 (\pm 0.3) \times 10^{-2}$	$5.2 \times 10^{-12}$	(a)
<i>n</i> -heptane	$5.5 (\pm 2.4) \times 10^{-3}$	$8.5 (\pm 3.0) \times 10^{-3}$	$7.9 (\pm 3.0) \times 10^{-3}$	$1.95 \times 10^{-17} T^2 \exp(406/T)$	(a)
cyclopentane	$4.9 (\pm 1.4) \times 10^{-3}$	$6.9 (\pm 2.4) \times 10^{-3}$	$7.8 (\pm 2.7) \times 10^{-3}$	$2.73 \times 10^{-17} T^2 \exp(214/T)$	(a)
2,3,4-trimethylpentane	$6.1 (\pm 2.3) \times 10^{-3}$	$7.2 (\pm 2.0) \times 10^{-3}$	$6.4 (\pm 2.3) \times 10^{-3}$	$6.6 \times 10^{-12}$	(a)
ethane*	$5.0 (\pm 2.3) \times 10^{-3}$	$5.0 (\pm 1.8) \times 10^{-3}$	$5.9 (\pm 2.1) \times 10^{-3}$	$1.49 \times 10^{-17} T^2 \exp(-499/T)$	(a)
isooctane	$4.2 (\pm 2.1) \times 10^{-3}$	$4.9 (\pm 1.3) \times 10^{-3}$	$4.7 (\pm 1.4) \times 10^{-3}$	$2.34 \times 10^{-17} T^2 \exp(140/T)$	(a)
2,3-dimethylpentane	$4.6 (\pm 2.6) \times 10^{-3}$	$4.6 (\pm 1.4) \times 10^{-3}$	$4.4 (\pm 1.5) \times 10^{-3}$	$4.77 \times 10^{-12}$	(a) <sup>2</sup>
2,4- and 2,2-dimethylpentane	$1.5 (\pm 0.3) \times 10^{-3}$	$2.3 (\pm 0.7) \times 10^{-3}$	$2.4 (\pm 0.7) \times 10^{-3}$	$4.77 \times 10^{-12}$	(a) <sup>2</sup>
2,2-dimethylbutane	$1.4 (\pm 0.3) \times 10^{-3}$	$2.2 (\pm 0.6) \times 10^{-3}$	$2.4 (\pm 0.7) \times 10^{-3}$	$3.37 \times 10^{-11} \exp(-809/T)$	(a)
3-methylheptane	$1.5 (\pm 0.3) \times 10^{-3}$	$1.8 (\pm 0.9) \times 10^{-3}$	$1.9 (\pm 0.9) \times 10^{-3}$	$6.0 \times 10^{-12}$	(**) <sup>3</sup>
2,4-dimethylhexane	$1.3 (\pm 0.5) \times 10^{-3}$	$1.5 (\pm 0.4) \times 10^{-3}$	$1.4 (\pm 0.5) \times 10^{-3}$	$6.0 \times 10^{-12}$	(**) <sup>3</sup>
2,2,5-trimethylhexane	$1.1 (\pm 0.6) \times 10^{-3}$	$1.2 (\pm 0.4) \times 10^{-3}$	$1.1 (\pm 0.4) \times 10^{-3}$	$6.0 \times 10^{-12}$	(**) <sup>3</sup>
3,3-dimethylpentane	$6.3 (\pm 3.0) \times 10^{-4}$	$9.2 (\pm 3.5) \times 10^{-4}$	$9.0 (\pm 2.9) \times 10^{-4}$	$6.0 \times 10^{-12}$	(**) <sup>3</sup>
2,2,3-trimethylpentane	$4.7 (\pm 3.0) \times 10^{-4}$	$6.9 (\pm 3.5) \times 10^{-4}$	$7.4 (\pm 3.4) \times 10^{-4}$	$6.0 \times 10^{-12}$	(**) <sup>3</sup>
2,2-dimethylhexane	$1.4 (\pm 0.2) \times 10^{-4}$	$1.6 (\pm 0.7) \times 10^{-4}$	$1.8 (\pm 0.4) \times 10^{-4}$	$6.0 \times 10^{-12}$	(**) <sup>3</sup>
2,2,5-trimethylheptane	$1.2 (\pm 0.3) \times 10^{-4}$	$1.2 (\pm 0.3) \times 10^{-4}$	$1.2 (\pm 0.4) \times 10^{-4}$	$6.0 \times 10^{-12}$	(**) <sup>3</sup>
C <sub>1</sub> -C <sub>3</sub> acids					
acetic acid	$1.2 (\pm 0.7) \times 10^{-2}$	$1.9 (\pm 1.0) \times 10^{-2}$	$2.7 (\pm 1.1) \times 10^{-2}$	$8.0 \times 10^{-13}$	(e)
formic acid	$4.1 (\pm 2.4) \times 10^{-3}$	$1.5 (\pm 0.6) \times 10^{-2}$	$2.6 (\pm 1.4) \times 10^{-2}$	$4.5 \times 10^{-13}$	(f)
propionic acid	$4.3 (\pm 1.7) \times 10^{-3}$	$6.3 (\pm 2.6) \times 10^{-3}$	$7.3 (\pm 2.1) \times 10^{-3}$	$1.2 \times 10^{-12}$	(f)
Temperature-independent AVOCs					
Temperature-independent alkanes					
cyclohexane	$8.3 (\pm 4.3) \times 10^{-3}$	$8.5 (\pm 6.1) \times 10^{-3}$	$8.6 (\pm 5.1) \times 10^{-3}$	$3.26 \times 10^{-17} T^2 \exp(262/T)$	(a)
methylcyclohexane	$8.7 (\pm 4.5) \times 10^{-3}$	$7.3 (\pm 2.7) \times 10^{-3}$	$6.8 (\pm 2.3) \times 10^{-3}$	$9.64 \times 10^{-12}$	(a)
3-methylhexane	$6.6 (\pm 3.4) \times 10^{-3}$	$6.1 (\pm 1.9) \times 10^{-3}$	$5.9 (\pm 1.8) \times 10^{-3}$	$6.3 \times 10^{-12}$	(d)
methyl ethyl ketone	$2.9 (\pm 1.8) \times 10^{-3}$	$3.7 (\pm 1.7) \times 10^{-3}$	$4.9 (\pm 3.3) \times 10^{-3}$	$1.32 \times 10^{-12} \exp(-25/T)$	(f)
2-methylhexane	$5.5 (\pm 3.2) \times 10^{-3}$	$5.7 (\pm 1.9) \times 10^{-3}$	$4.6 (\pm 1.9) \times 10^{-3}$	$6.69 \times 10^{-12}$	(d)
<i>trans</i> -1,3-dimethylcyclopentane	$4.5 (\pm 3.1) \times 10^{-3}$	$5.0 (\pm 3.6) \times 10^{-3}$	$4.4 (\pm 2.5) \times 10^{-3}$	$7.66 \times 10^{-12}$	(**) <sup>4</sup>
<i>cis</i> -1,3-dimethylcyclopentane	$4.6 (\pm 2.5) \times 10^{-3}$	$4.3 (\pm 1.6) \times 10^{-3}$	$4.0 (\pm 1.5) \times 10^{-3}$	$7.66 \times 10^{-12}$	(**) <sup>4</sup>
2,3,3-trimethylpentane and 2,3-dimethylhexane	$2.6 (\pm 1.6) \times 10^{-3}$	$2.8 (\pm 0.9) \times 10^{-3}$	$2.3 (\pm 1.0) \times 10^{-3}$	$6.0 \times 10^{-12}$	(**) <sup>3</sup>
<i>n</i> -undecane	$2.7 (\pm 1.1) \times 10^{-3}$	$2.4 (\pm 1.0) \times 10^{-3}$	$2.2 (\pm 1.2) \times 10^{-3}$	$12.3 \times 10^{-12}$	(a)
<i>n</i> -decane	$3.2 (\pm 2.1) \times 10^{-3}$	$2.3 (\pm 0.7) \times 10^{-3}$	$2.0 (\pm 0.8) \times 10^{-3}$	$11.0 \times 10^{-12}$	(a)
2-methylheptane	$2.3 (\pm 1.2) \times 10^{-3}$	$2.1 (\pm 0.6) \times 10^{-3}$	$2.0 (\pm 0.6) \times 10^{-3}$	$6.0 \times 10^{-12}$	(**) <sup>3</sup>

## Temperature dependent impacts of emission controls

S. E. Pusede et al.

Title Page

Abstract

Introduction

Conclusions

References

Tables

Figures

◀

▶

◀

▶

Back

Close

Full Screen / Esc

Printer-friendly Version

Interactive Discussion



Table A2. Continued.

Species	Mean ( $\pm 1\sigma$ ) VOCR ( $\text{s}^{-1}$ ) by temperature			$k$ or $k(T)$ ( $\text{cm}^3 \text{molecule}^{-1} \text{s}^{-1}$ )	Reference
	Low	Moderate	High		
ethylcyclopentane	$2.5 (\pm 1.1) \times 10^{-3}$	$2.0 (\pm 0.7) \times 10^{-3}$	$1.9 (\pm 0.7) \times 10^{-3}$	$7.66 \times 10^{-12}$	(**) <sup>4</sup>
<i>n</i> -dodecane	$1.6 (\pm 0.7) \times 10^{-3}$	$1.6 (\pm 0.6) \times 10^{-3}$	$1.5 (\pm 0.7) \times 10^{-3}$	$13.2 \times 10^{-12}$	(a)
<i>cis,trans,cis</i> -1,2,4-trimethylcyclopentane	$1.8 (\pm 1.5) \times 10^{-3}$	$1.7 (\pm 0.5) \times 10^{-3}$	$1.5 (\pm 0.7) \times 10^{-3}$	$8.0 \times 10^{-12}$	(**) <sup>5</sup>
<i>cis</i> -1,3- and 1,1-dimethylcyclohexane	$2.1 (\pm 1.3) \times 10^{-3}$	$1.6 (\pm 0.6) \times 10^{-3}$	$1.5 (\pm 0.5) \times 10^{-3}$	$1.0 \times 10^{-11}$	(**) <sup>6</sup>
<i>n</i> -nonane	$2.5 (\pm 1.1) \times 10^{-3}$	$1.8 (\pm 0.6) \times 10^{-3}$	$1.5 (\pm 0.6) \times 10^{-3}$	$2.53 \times 10^{-17} T^2 \exp(436/T)$	(a)
ethylcyclohexane	$2.0 (\pm 1.2) \times 10^{-3}$	$1.7 (\pm 0.6) \times 10^{-3}$	$1.4 (\pm 0.5) \times 10^{-3}$	$1.0 \times 10^{-11}$	(**) <sup>6</sup>
<i>trans</i> -1,2-dimethylcyclohexane	$2.2 (\pm 1.5) \times 10^{-3}$	$1.7 (\pm 0.6) \times 10^{-3}$	$1.4 (\pm 0.6) \times 10^{-3}$	$1.0 \times 10^{-11}$	(**) <sup>6</sup>
<i>n</i> -tetradecane	$1.6 (\pm 0.6) \times 10^{-3}$	$1.5 (\pm 0.5) \times 10^{-3}$	$1.3 (\pm 0.4) \times 10^{-3}$	$1.79 \times 10^{-11}$	(a)
<i>n</i> -tridecane	$1.8 (\pm 0.5) \times 10^{-3}$	$1.7 (\pm 0.5) \times 10^{-3}$	$1.2 (\pm 0.5) \times 10^{-3}$	$15.1 \times 10^{-12}$	(a)
2,5-dimethylhexane	$1.4 (\pm 0.8) \times 10^{-3}$	$1.3 (\pm 0.4) \times 10^{-3}$	$1.2 (\pm 0.4) \times 10^{-3}$	$6.0 \times 10^{-12}$	(**) <sup>3</sup>
<i>trans</i> -1,3-dimethylcyclohexane	$1.2 (\pm 0.7) \times 10^{-3}$	$9.5 (\pm 2.9) \times 10^{-4}$	$8.4 (\pm 2.9) \times 10^{-4}$	$1.0 \times 10^{-11}$	(**) <sup>6</sup>
2,6-dimethylheptane	$1.2 (\pm 0.6) \times 10^{-3}$	$1.0 (\pm 0.4) \times 10^{-3}$	$8.3 (\pm 4.4) \times 10^{-4}$	$6.0 \times 10^{-12}$	(**) <sup>3</sup>
1,1,3-trimethylcyclohexane	$1.2 (\pm 0.9) \times 10^{-3}$	$9.3 (\pm 3.9) \times 10^{-4}$	$7.8 (\pm 2.8) \times 10^{-4}$	$1.0 \times 10^{-11}$	(**) <sup>6</sup>
4-methylheptane	$1.6 (\pm 1.3) \times 10^{-3}$	$9.4 (\pm 6.6) \times 10^{-4}$	$7.4 (\pm 2.6) \times 10^{-4}$	$6.0 \times 10^{-12}$	(**) <sup>3</sup>
<i>cis</i> -1,2-dimethylcyclohexane	$7.0 (\pm 3.3) \times 10^{-4}$	$5.6 (\pm 1.5) \times 10^{-4}$	$5.7 (\pm 1.9) \times 10^{-4}$	$1.0 \times 10^{-11}$	(**) <sup>6</sup>
3-methyloctane and 4-ethylheptane	$6.9 (\pm 3.0) \times 10^{-4}$	$6.2 (\pm 2.0) \times 10^{-4}$	$5.5 (\pm 2.1) \times 10^{-4}$	$6.0 \times 10^{-12}$	(**) <sup>3</sup>
2- and 4-methyloctane	$6.6 (\pm 3.2) \times 10^{-4}$	$5.3 (\pm 1.6) \times 10^{-4}$	$5.2 (\pm 1.9) \times 10^{-4}$	$8.0 \times 10^{-12}$	(**) <sup>3</sup>
<i>n</i> -propylcyclopentane	$5.3 (\pm 2.4) \times 10^{-4}$	$5.2 (\pm 1.7) \times 10^{-4}$	$4.7 (\pm 1.0) \times 10^{-4}$	$6.0 \times 10^{-12}$	(**) <sup>5</sup>
1,1,4-trimethylcyclohexane	$5.1 (\pm 5.5) \times 10^{-4}$	$4.4 (\pm 1.5) \times 10^{-4}$	$4.4 (\pm 2.9) \times 10^{-4}$	$1.0 \times 10^{-11}$	(**) <sup>6</sup>
<i>cis,trans,cis</i> -1,2,4-trimethylcyclohexane	$5.9 (\pm 4.2) \times 10^{-4}$	$4.1 (\pm 1.0) \times 10^{-4}$	$3.7 (\pm 1.9) \times 10^{-4}$	$1.0 \times 10^{-11}$	(**) <sup>6</sup>
3,5-dimethylheptane	$4.8 (\pm 2.2) \times 10^{-4}$	$4.1 (\pm 1.3) \times 10^{-4}$	$3.6 (\pm 1.1) \times 10^{-4}$	$6.0 \times 10^{-12}$	(**) <sup>3</sup>
<i>cis,trans,trans</i> -1,2,4- and <i>cis,cis,trans</i> -1,3,5-trimethylhexane	$2.0 (\pm 1.3) \times 10^{-4}$	$1.8 (\pm 1.1) \times 10^{-4}$	$3.1 (\pm 3.1) \times 10^{-4}$	$1.0 \times 10^{-11}$	(**) <sup>6</sup>
<i>cis,cis,cis</i> -1,3,5-trimethylcyclohexane	$3.9 (\pm 2.7) \times 10^{-4}$	$3.3 (\pm 1.1) \times 10^{-4}$	$2.9 (\pm 1.7) \times 10^{-4}$	$1.0 \times 10^{-11}$	(**) <sup>6</sup>
isopropylcyclopentane	$2.7 (\pm 1.3) \times 10^{-4}$	$2.4 (\pm 0.6) \times 10^{-4}$	$2.4 (\pm 1.3) \times 10^{-4}$	$8.0 \times 10^{-12}$	(**) <sup>5</sup>
2,3-dimethylheptane	$1.7 (\pm 0.6) \times 10^{-4}$	$1.6 (\pm 0.5) \times 10^{-4}$	$1.5 (\pm 0.4) \times 10^{-4}$	$6.0 \times 10^{-12}$	(**) <sup>3</sup>
2,2,4-trimethylheptane	$1.5 (\pm 0.6) \times 10^{-4}$	$1.6 (\pm 0.4) \times 10^{-4}$	$1.5 (\pm 0.3) \times 10^{-4}$	$6.0 \times 10^{-12}$	(**) <sup>3</sup>
Alkenes					
propene	$9.0 (\pm 4.7) \times 10^{-2}$	$6.5 (\pm 2.4) \times 10^{-2}$	$5.5 (\pm 1.5) \times 10^{-2}$	$4.85 \times 10^{-12} \exp(504/T)$	(a)
<i>cis</i> -2-pentene	$2.5 (\pm 1.1) \times 10^{-2}$	$3.0 (\pm 0.9) \times 10^{-2}$	$3.8 (\pm 1.9) \times 10^{-2}$	$6.50 \times 10^{-11}$	(a)
1-butene and isobutene	$4.7 (\pm 2.0) \times 10^{-2}$	$3.6 (\pm 1.4) \times 10^{-2}$	$3.1 (\pm 1.1) \times 10^{-2}$	$6.55 \times 10^{-12} \exp(467/T)$	(**) <sup>7</sup>
<i>cis</i> -2-butene	$1.5 (\pm 0.1) \times 10^{-2}$	$1.3 (\pm 0.6) \times 10^{-2}$	$1.6 (\pm 0.3) \times 10^{-2}$	$1.1 \times 10^{-11} \exp(487/T)$	(a)
1-hexene	$1.8 (\pm 0.7) \times 10^{-2}$	$1.2 (\pm 0.4) \times 10^{-2}$	$1.4 (\pm 0.3) \times 10^{-2}$	$3.70 \times 10^{-11}$	(a)
1-pentene	$2.4 (\pm 1.4) \times 10^{-2}$	$1.1 (\pm 0.3) \times 10^{-2}$	$1.4 (\pm 0.2) \times 10^{-2}$	$3.14 \times 10^{-11}$	(a)
cyclopentene	$1.3 (\pm 0.7) \times 10^{-2}$	$1.2 (\pm 0.4) \times 10^{-2}$	$1.2 (\pm 0.5) \times 10^{-2}$	$6.70 \times 10^{-11}$	(a)
<i>trans</i> -2-butene	$1.2 (\pm 0.4) \times 10^{-2}$	$1.1 (\pm 0.3) \times 10^{-2}$	$1.0 (\pm 0.3) \times 10^{-2}$	$1.01 \times 10^{-11} \exp(550/T)$	(a)
2-methyl-2- and <i>cis</i> -3-methyl-2-pentene	$3.0 (\pm 1.5) \times 10^{-3}$	$2.5 (\pm 0.6) \times 10^{-3}$	$3.2 (\pm 0.8) \times 10^{-3}$	$8.90 \times 10^{-11}$	(**) <sup>8</sup>
1-methylcyclohexene	$2.0 (\pm 0.1) \times 10^{-3}$	$1.7 (\pm 0.5) \times 10^{-3}$	$1.5 (\pm 0.4) \times 10^{-3}$	$8.90 \times 10^{-11}$	(**) <sup>8</sup>

## Temperature dependent impacts of emission controls

S. E. Pusede et al.

Title Page

Abstract

Introduction

Conclusions

References

Tables

Figures

◀

▶

◀

▶

Back

Close

Full Screen / Esc

Printer-friendly Version

Interactive Discussion



## Temperature dependent impacts of emission controls

S. E. Pusede et al.

Title Page

Abstract

Introduction

Conclusions

References

Tables

Figures

◀

▶

◀

▶

Back

Close

Full Screen / Esc

Printer-friendly Version

Interactive Discussion

Table A2. Continued.

Species	Mean ( $\pm 1\sigma$ ) VOCR ( $s^{-1}$ ) by temperature			$k$ or $k(T)$ ( $cm^3 molecule^{-1} s^{-1}$ )	Reference
	Low	Moderate	High		
<i>m</i> - and <i>p</i> -xylene	$3.5 (\pm 2.0) \times 10^{-2}$	$3.0 (\pm 1.0) \times 10^{-2}$	$2.5 (\pm 1.1) \times 10^{-2}$	$1.87 \times 10^{-11}$	(a) <sup>9</sup>
toluene	$2.9 (\pm 1.3) \times 10^{-2}$	$2.6 (\pm 0.8) \times 10^{-2}$	$2.2 (\pm 0.7) \times 10^{-2}$	$1.18 \times 10^{-12} \exp(338/T)$	(a)
phenol	$4.2 (\pm 5.7) \times 10^{-2}$	$1.7 (\pm 0.7) \times 10^{-2}$	$1.3 (\pm 0.2) \times 10^{-2}$	$2.70 \times 10^{-11}$	(g)
1,2,4-trimethylbenzene	$1.6 (\pm 1.0) \times 10^{-2}$	$1.4 (\pm 0.5) \times 10^{-2}$	$1.2 (\pm 0.5) \times 10^{-2}$	$3.25 \times 10^{-11}$	(a)
1,3,5-trimethylbenzene	$9.4 (\pm 6.3) \times 10^{-3}$	$8.4 (\pm 3.5) \times 10^{-3}$	$7.3 (\pm 5.1) \times 10^{-3}$	$5.67 \times 10^{-11}$	(a)
<i>o</i> -xylene	$9.2 (\pm 5.1) \times 10^{-3}$	$8.5 (\pm 3.1) \times 10^{-3}$	$7.1 (\pm 3.0) \times 10^{-3}$	$1.36 \times 10^{-11}$	(a)
<i>m</i> - and <i>p</i> -ethyltoluene	$7.5 (\pm 4.5) \times 10^{-3}$	$5.8 (\pm 2.2) \times 10^{-3}$	$5.0 (\pm 2.5) \times 10^{-3}$	$1.87 \times 10^{-11}$	(a) <sup>10</sup>
ethylbenzene	$4.6 (\pm 2.9) \times 10^{-3}$	$4.1 (\pm 1.4) \times 10^{-3}$	$3.4 (\pm 1.2) \times 10^{-3}$	$7.0 \times 10^{-12}$	(a)
1,2,3-trimethylbenzene	$4.8 (\pm 2.3) \times 10^{-3}$	$3.8 (\pm 1.2) \times 10^{-3}$	$3.3 (\pm 1.4) \times 10^{-3}$	$3.27 \times 10^{-11}$	(a)
benzene*	$2.9 (\pm 1.3) \times 10^{-3}$	$2.6 (\pm 0.8) \times 10^{-3}$	$2.2 (\pm 0.7) \times 10^{-3}$	$2.33 \times 10^{-12} \exp(-193/T)$	(a)
<i>o</i> -ethyltoluene	$1.7 (\pm 0.8) \times 10^{-3}$	$1.4 (\pm 0.5) \times 10^{-3}$	$1.2 (\pm 0.5) \times 10^{-3}$	$1.19 \times 10^{-11}$	(a)
Aromatics					
<i>p</i> -diethylbenzene	$7.0 (\pm 2.4) \times 10^{-4}$	$6.9 (\pm 2.3) \times 10^{-4}$	$6.3 (\pm 3.0) \times 10^{-4}$	$8.11 \times 10^{-12}$	(h)
<i>n</i> -propylbenzene	$7.5 (\pm 3.1) \times 10^{-4}$	$7.2 (\pm 2.3) \times 10^{-4}$	$6.2 (\pm 2.0) \times 10^{-4}$	$5.8 \times 10^{-12}$	(a)
1-methyl-3- <i>n</i> -propyl benzene	$8.4 (\pm 2.8) \times 10^{-4}$	$8.4 (\pm 3.8) \times 10^{-4}$	$6.2 (\pm 2.7) \times 10^{-4}$	$1.0 \times 10^{-11}$	(**) <sup>11</sup>
<i>m</i> -diethylbenzene	$5.6 (\pm 2.5) \times 10^{-4}$	$6.4 (\pm 2.2) \times 10^{-4}$	$6.2 (\pm 2.2) \times 10^{-4}$	$1.0 \times 10^{-11}$	(**) <sup>11</sup>
<i>p</i> -cymene	$5.5 (\pm 2.8) \times 10^{-4}$	$5.6 (\pm 1.5) \times 10^{-4}$	$5.7 (\pm 1.8) \times 10^{-4}$	$1.0 \times 10^{-11}$	(**) <sup>11</sup>
1,3-dimethyl-4-ethylbenzene	$3.4 (\pm 1.6) \times 10^{-4}$	$2.5 (\pm 0.7) \times 10^{-4}$	$1.9 (\pm 0.8) \times 10^{-4}$	$1.0 \times 10^{-11}$	(**) <sup>11</sup>
1,4-dimethyl-2-ethyl benzene	$3.4 (\pm 1.8) \times 10^{-4}$	$2.2 (\pm 0.7) \times 10^{-4}$	$1.9 (\pm 0.8) \times 10^{-4}$	$1.0 \times 10^{-11}$	(**) <sup>11</sup>
isobutylbenzene	$1.6 (\pm 0.7) \times 10^{-4}$	$1.4 (\pm 0.4) \times 10^{-4}$	$1.7 (\pm 0.7) \times 10^{-4}$	$1.0 \times 10^{-11}$	(**) <sup>11</sup>
1,2-dimethyl-4-ethylbenzene	$2.3 (\pm 1.3) \times 10^{-4}$	$1.9 (\pm 0.5) \times 10^{-4}$	$1.6 (\pm 0.6) \times 10^{-4}$	$1.0 \times 10^{-11}$	(**) <sup>11</sup>
1,2,3,5-tetramethylbenzene	$1.7 (\pm 0.5) \times 10^{-4}$	$1.5 (\pm 0.4) \times 10^{-4}$	$1.6 (\pm 0.5) \times 10^{-4}$	$1.0 \times 10^{-11}$	(**) <sup>11</sup>
<i>m</i> -cymene	$3.2 (\pm 2.0) \times 10^{-4}$	$1.4 (\pm 0.3) \times 10^{-4}$	$1.5 (\pm 0.6) \times 10^{-4}$	$1.0 \times 10^{-11}$	(**) <sup>11</sup>
<i>n</i> -butylbenzene	$2.6 (\pm 2.6) \times 10^{-4}$	$1.7 (\pm 0.3) \times 10^{-4}$	$1.5 (\pm 0.5) \times 10^{-4}$	$1.0 \times 10^{-11}$	(**) <sup>11</sup>
1-methyl-2- <i>n</i> -propyl benzene	$2.2 (\pm 0.9) \times 10^{-4}$	$1.8 (\pm 0.4) \times 10^{-4}$	$1.5 (\pm 0.4) \times 10^{-4}$	$1.0 \times 10^{-11}$	(**) <sup>11</sup>
1,2-dimethyl-3-ethylbenzene	$2.6 (\pm 0.9) \times 10^{-4}$	$1.5 (\pm 0.3) \times 10^{-4}$	$1.4 (\pm 0.3) \times 10^{-4}$	$1.0 \times 10^{-11}$	(**) <sup>11</sup>
1,2,4,5-tetramethylbenzene	$1.8 (\pm 0.6) \times 10^{-4}$	$1.4 (\pm 0.3) \times 10^{-4}$	$1.4 (\pm 0.2) \times 10^{-4}$	$1.0 \times 10^{-11}$	(**) <sup>11</sup>
1,2,3,4-tetramethylbenzene	$1.5 (\pm 0.2) \times 10^{-4}$	$1.3 (\pm 0.3) \times 10^{-4}$	$1.4 (\pm 0.3) \times 10^{-4}$	$1.0 \times 10^{-11}$	(**) <sup>11</sup>



## Temperature dependent impacts of emission controls

S. E. Pusede et al.

Table A2. Continued.

Species	Mean ( $\pm 1\sigma$ ) VOCR ( $s^{-1}$ ) by temperature			$k$ or $k(T)$ ( $cm^3 \text{ molecule}^{-1} s^{-1}$ )	Reference
	Low	Moderate	High		
Aldehydes and ketones					
nonanal	$2.6 (\pm 1.5) \times 10^{-1}$	$1.7 (\pm 1.2) \times 10^{-1}$	$1.5 (\pm 0.4) \times 10^{-1}$	$3.0 \times 10^{-11}$	(**) <sup>12</sup>
heptanal	$1.7 (\pm 0.6) \times 10^{-1}$	$1.1 (\pm 0.5) \times 10^{-1}$	$7.9 (\pm 3.0) \times 10^{-2}$	$3.0 \times 10^{-11}$	(a)
hexanal	$1.1 (\pm 3.3) \times 10^{-1}$	$7.2 (\pm 2.6) \times 10^{-2}$	$6.6 (\pm 1.5) \times 10^{-2}$	$3.0 \times 10^{-11}$	(a)
pentanal	$4.3 (\pm 1.6) \times 10^{-2}$	$3.9 (\pm 1.7) \times 10^{-2}$	$3.7 (\pm 1.0) \times 10^{-2}$	$9.9 \times 10^{-11} \exp(310/T)$	(a)
butanal	$2.6 (\pm 1.2) \times 10^{-2}$	$2.7 (\pm 0.6) \times 10^{-2}$	$3.2 (\pm 0.9) \times 10^{-2}$	$6.0 \times 10^{-12} \exp(410/T)$	(a)
propanal	$2.6 (\pm 1.2) \times 10^{-2}$	$3.4 (\pm 2.2) \times 10^{-2}$	$2.3 (\pm 0.9) \times 10^{-2}$	$5.1 \times 10^{-12} \exp(405/T)$	(a)
methyl isobutyl ketone	$2.2 (\pm 0.7) \times 10^{-3}$	$2.4 (\pm 1.5) \times 10^{-3}$	$2.5 (\pm 0.7) \times 10^{-3}$	$1.3 \times 10^{-11}$	(a)
acetophenone	$1.7 (\pm 0.9) \times 10^{-3}$	$1.4 (\pm 0.6) \times 10^{-3}$	$1.3 (\pm 0.4) \times 10^{-3}$	$1.0 \times 10^{-11}$	(**) <sup>11</sup>
methyl <i>n</i> -butyl ketone	$1.1 (\pm 0.5) \times 10^{-3}$	$1.3 (\pm 0.4) \times 10^{-3}$	$1.2 (\pm 0.2) \times 10^{-3}$	$9.1 \times 10^{-12}$	(a)
CO					
CO	$8.9 (\pm 1.0) \times 10^{-1}$	$8.9 (\pm 1.2) \times 10^{-1}$	$8.5 (\pm 1.4) \times 10^{-1}$	$2.4 \times 10^{-13}$	(i) <sup>13</sup>

<sup>a</sup>Atkinson and Arey (2003), <sup>b</sup>Dillion et al. (2004), <sup>c</sup>Yamada et al. (2003), <sup>d</sup>Sprengnether et al. (2009), <sup>e</sup>Atkinson et al. (1992), <sup>f</sup>Atkinson et al. (2001),

<sup>g</sup>Calvert et al. (2002), <sup>h</sup>Atkinson et al. (1994), <sup>i</sup>Sander et al. (2003)

<sup>1</sup> Rate expression is for 2-methylpentane + OH. <sup>2</sup> Rate expression is for 2,4-dimethylpentane + OH. <sup>3</sup> Value is generic for  $\sim C_7$  + OH at 298 K. <sup>4</sup> Rate constant is for ethylcyclopentane + OH at 298 K. <sup>5</sup> Value is generic for  $\sim C_8$  + OH at 298 K. <sup>6</sup> Value is generic for branched  $\sim C_7$  cycloalkane + OH at 298 K.

<sup>7</sup> Rate expression is for 1-butene + OH. <sup>8</sup> Rate constant is for cyclohexene + OH at 298 K. <sup>9</sup> Rate constant is an average of *m*- and *p*-xylene + OH at 298 K. <sup>10</sup> Rate constant is an average of *m*- and *p*-ethyltoluene + OH at 298 K. <sup>11</sup> Value is generic for an aromatic + OH at 298 K. <sup>12</sup> Rate constant is for heptanal + OH at 298 K. <sup>13</sup> Listed value is at 298 K. In our analysis we use the CO + OH formulation given in Sander et al. (2003).

Title Page

Abstract

Introduction

Conclusions

References

Tables

Figures

◀

▶

◀

▶

Back

Close

Full Screen / Esc

Printer-friendly Version

Interactive Discussion

## Temperature dependent impacts of emission controls

S. E. Pusede et al.

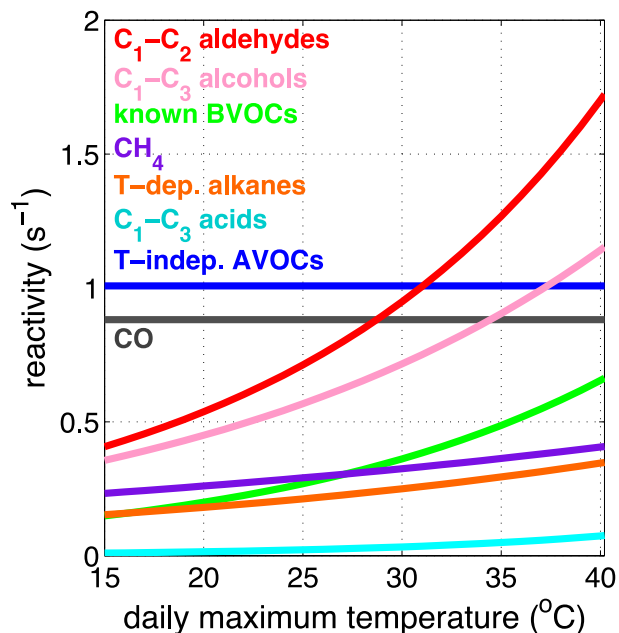


**Fig. 1.** Empirical fits of the daily average (10 a.m.–2 p.m. LT)  $\sum_i \text{VOCR}_i$  ( $\text{s}^{-1}$ ) vs. daily maximum temperature ( $^{\circ}\text{C}$ ) (data points for each curve are shown in Fig. A1). Colors are as follows:  $\text{C}_1$ – $\text{C}_2$  aldehydes (red),  $\text{C}_1$ – $\text{C}_3$  alcohols (pink), known-biogenic VOCs (green),  $\text{CH}_4$  (purple), temperature-dependent alkanes (orange),  $\text{C}_1$ – $\text{C}_3$  organic acids (cyan), temperature-independent AVOCs (blue), and CO (gray). For a listing of the mean  $\text{VOCR}_i$  of each molecule see Table A2.

[Title Page](#)
[Abstract](#)
[Introduction](#)
[Conclusions](#)
[References](#)
[Tables](#)
[Figures](#)
[◀](#)
[▶](#)
[◀](#)
[▶](#)
[Back](#)
[Close](#)
[Full Screen / Esc](#)
[Printer-friendly Version](#)
[Interactive Discussion](#)


## Temperature dependent impacts of emission controls

S. E. Pusede et al.

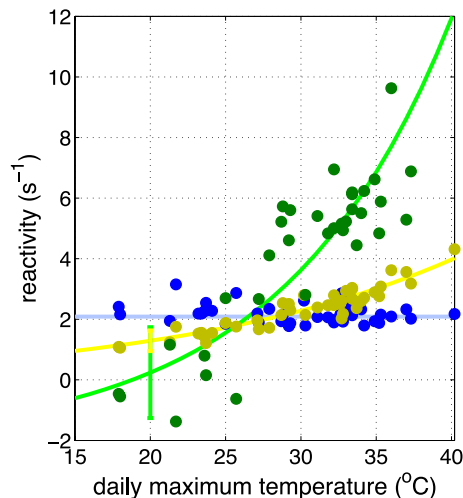


**Fig. 2.** Daily average (10 a.m.–2 p.m. LT) organic reactivity ( $\text{s}^{-1}$ ) vs. the daily maximum temperature ( $^{\circ}\text{C}$ ) with fits: temperature-independent  $\sum_i \text{VOCR}_i$  (blue), temperature-dependent  $\sum_i \text{VOCR}_i$  (yellow), and temperature-dependent VOCR (green). The temperature-dependent VOCR is equal to the measured OH reactivity minus the temperature-independent  $\sum_i \text{VOCR}_i$  and minus the OH reactivities of  $\text{NO}_2$ , NO, HONO,  $\text{HNO}_3$ ,  $\text{NH}_3$ , and  $\text{SO}_2$ . The mean temperature-independent  $\sum_i \text{VOCR}_i$  is  $2.1 \pm 0.3_1$  ( $1\sigma$ ) (light blue line). The unknown reactivity is thus temperature-dependent and is the difference between the yellow and green curves. The error bars are the sum of the squared  $y$  residuals divided by (the number of points less 2) and are  $\pm 0.3_4$  (yellow) and  $\pm 1.5$  (green).

Title Page

Abstract

Introduction

Conclusions

References

Tables

Figures

◀

▶

◀

▶

Back

Close

Full Screen / Esc

Printer-friendly Version

Interactive Discussion



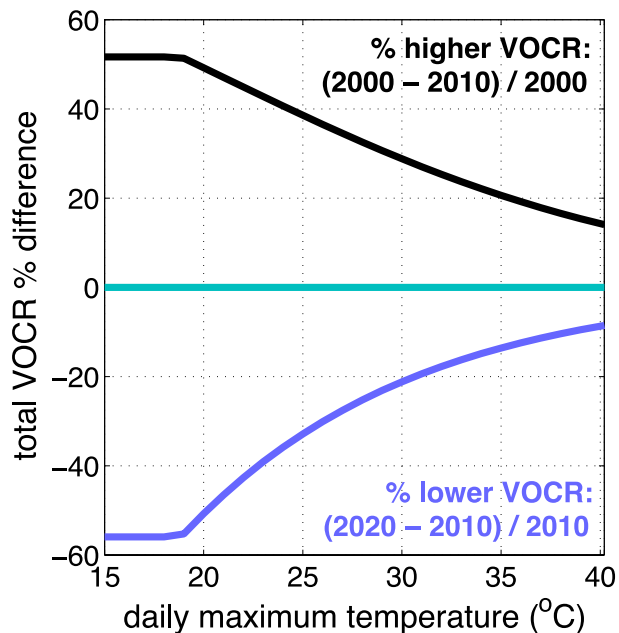


**Fig. 3.** The effects of organic emissions reductions on the total VOCR vs. daily maximum temperature ( $^{\circ}\text{C}$ ). We assume here that the temperature-independent  $\sum_i \text{VOCR}_i$  ( $2.1 \text{ s}^{-1}$ ) has decreased and will continue to decrease at rate of  $6\% \text{ yr}^{-1}$  and that the temperature-dependent reactivity has been and will continue to be unchanged. The percent difference (higher) in the total VOCR in 2000,  $(\text{VOCR}_{2000} - \text{VOCR}_{2010})/\text{VOCR}_{2000}$ , is in black. The percent change (lower) in the total VOCR in 2020,  $(\text{VOCR}_{2020} - \text{VOCR}_{2010})/\text{VOCR}_{2010}$ , is in periwinkle. The turquoise line is the year 2010 at 0%.

Temperature dependent impacts of emission controls

S. E. Pusede et al.

Title Page

Abstract Introduction

Conclusions References

Tables Figures

◀ ▶

◀ ▶

Back Close

Full Screen / Esc

Printer-friendly Version

Interactive Discussion



## Temperature dependent impacts of emission controls

S. E. Pusede et al.

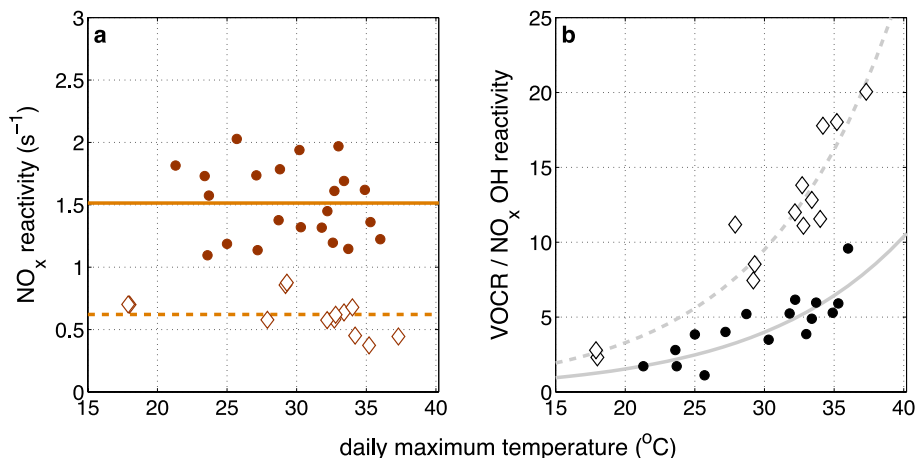


**Fig. 4. (a):** daily average (10 a.m.–2 p.m. LT)  $\text{NO}_x\text{R}$  ( $\text{s}^{-1}$ ) vs. the daily maximum temperature ( $^{\circ}\text{C}$ ) separated by weekdays (closed circles) and weekends (open diamonds). Weekdays are Tuesdays–Fridays. Weekends are Saturdays, Sundays, and Memorial Day (31 May 2010). Mondays and Saturdays are considered transition days, as they are influenced by carryover from the previous day. We omit Mondays for this reason but retain Saturdays to improve weekend statistics. The solid line is the weekday average value of  $1.5\text{ s}^{-1}$  and the dashed line is the weekend average value of  $0.6\text{ s}^{-1}$ . **(b):** total VOCR per unit  $\text{NO}_x\text{R}$  for weekdays (closed circles) and weekends (open diamond) vs. the daily maximum temperature ( $^{\circ}\text{C}$ ). The curves are exponential fits to the weekday (solid gray line) and weekend (dashed gray line) data.

[Title Page](#)
[Abstract](#)
[Introduction](#)
[Conclusions](#)
[References](#)
[Tables](#)
[Figures](#)
[◀](#)
[▶](#)
[◀](#)
[▶](#)
[Back](#)
[Close](#)
[Full Screen / Esc](#)
[Printer-friendly Version](#)
[Interactive Discussion](#)

## Temperature dependent impacts of emission controls

S. E. Pusede et al.

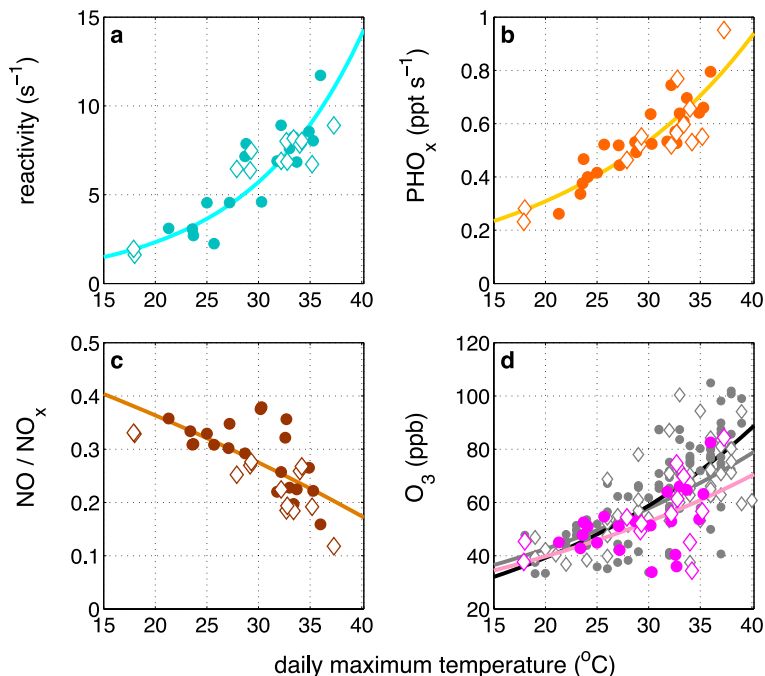


**Fig. 5.** (a) Total VOCR ( $\text{s}^{-1}$ ) (measured OH reactivity minus the OH reactivity contributions of  $\text{NO}_2$ , NO, HONO,  $\text{HNO}_3$ ,  $\text{NH}_3$ , and  $\text{SO}_2$ ). (b)  $\text{PHO}_x$  ( $\text{ppt s}^{-1}$ ). (c)  $\text{NO}/\text{NO}_x$ . (d)  $\text{O}_3$  (ppb) during CalNex-SJV (magenta) and in Bakersfield during the entire 2010  $\text{O}_3$  season (gray). All data are daily averages (10 a.m.–2 p.m. LT) vs. daily maximum temperature ( $^{\circ}\text{C}$ ), are shown for weekdays (closed circles) and weekends (open diamonds), and include their exponential fits. The 2010 Bakersfield  $\text{O}_3$  data are fit separately for weekdays (solid black line) and weekends (solid gray line).

[Title Page](#)
[Abstract](#)
[Introduction](#)
[Conclusions](#)
[References](#)
[Tables](#)
[Figures](#)
[◀](#)
[▶](#)
[◀](#)
[▶](#)
[Back](#)
[Close](#)
[Full Screen / Esc](#)
[Printer-friendly Version](#)
[Interactive Discussion](#)


## Temperature dependent impacts of emission controls

S. E. Pusede et al.

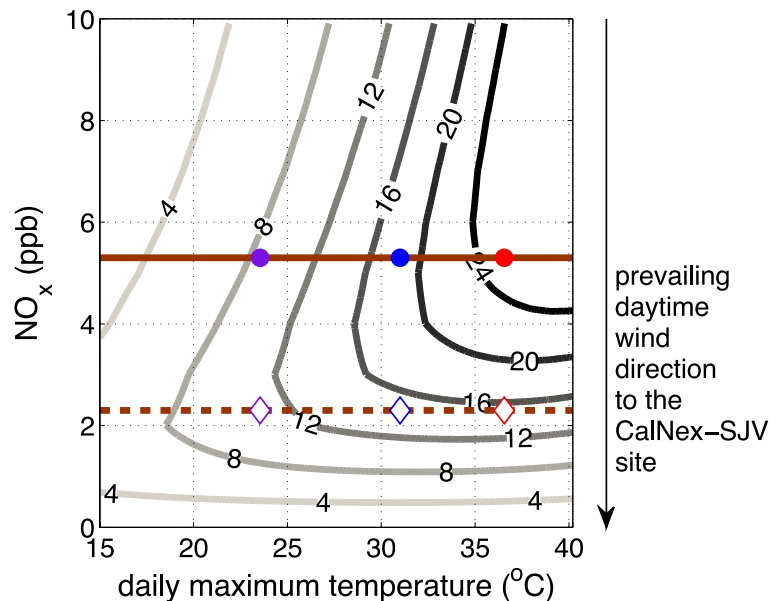


**Fig. 6.**  $PO_3$  at 4, 8, 12, 16, 20, and 24 ppbh<sup>-1</sup> as a function of  $NO_x$  mixing ratio vs. the daily maximum temperature (°C). Temperature here is a surrogate for VOCR.  $PO_3$  is calculated with an analytical model constrained with the CalNex-SJV observations (see text for details).  $NO_x$  (ppb) is shown for weekdays (solid brown line) and weekends (dashed brown line). The equivalent  $NO_xR$  are 1.5 and 0.6 s<sup>-1</sup>, respectively. The symbols are the  $NO_x$  mixing ratio at the 2010-average low (purple), moderate (blue), and high (red) temperatures on weekdays (closed circles) and weekends (open diamonds) for reference. The arrow along the right hand side represents the prevailing daytime (10 a.m.–2 p.m. LT) wind direction with respect to  $NO_x$  to the CalNex-SJV site.



## Temperature dependent impacts of emission controls

S. E. Pusede et al.

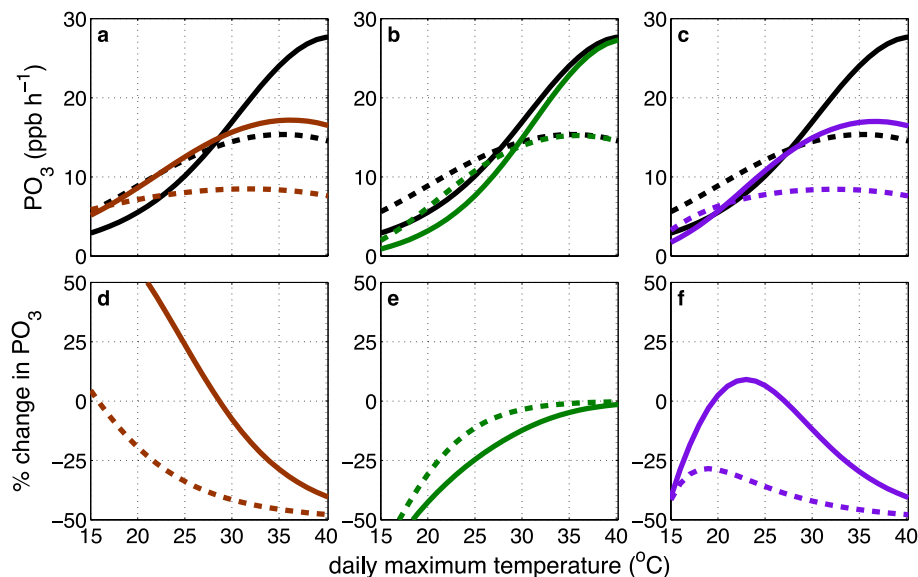


**Fig. 7. (a–c):**  $PO_3$  ( $ppb\ h^{-1}$ ) on weekdays (solid line) and weekends (dashed line) vs. daily maximum temperature ( $^{\circ}C$ ) calculated with CalNex-SJV observations (black) and in (a) with a 50%  $NO_x$  reduction (brown), in (b) with a 50% reduction in the temperature-independent  $\sum_i VO_{CR}_i$  (green), and in (c) with both reductions applied (purple). (d–f): the percent change between  $PO_3$  on weekdays (solid line) and weekends (dashed line) during CalNex-SJV and that computed after emission reduction vs. daily maximum temperature ( $^{\circ}C$ ).

Temperature  
dependent impacts of  
emission controls

S. E. Pusede et al.

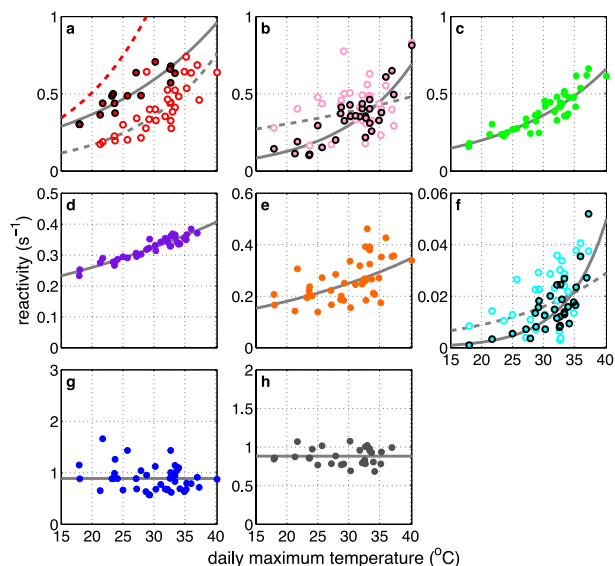


**Fig. A1.** Daily average  $\sum_i \text{VOCR}_i$  ( $\text{s}^{-1}$ ) vs. the daily maximum temperature ( $^{\circ}\text{C}$ ) for: **(a)**  $\text{H}_2\text{CO}$  (closed circles with black outline) and calculated acetaldehyde (open circles), **(b)** methanol (closed circles with black outline) and ethanol (open circles), **(c)** known-biogenic VOCs, **(d)**  $\text{CH}_4$ , **(e)** temperature-dependent alkanes, **(f)** formic acid (closed circles with black outline) and acetic acid (open circles), **(g)** all temperature-independent AVOCs, and **(h)** CO. Gray solid and dashed lines are empirically derived exponential fits for **(a–f)**. The solid lines in **(a)**, **(b)**, **(f)** are fits to the  $\text{C}_1$  molecules; the dashed lines are fits to the  $\text{C}_2$  molecules. In **(g)** and **(h)**, gray lines are means. Acetaldehyde, MVK, ethane, and benzene are estimated (see Appendix A for details), otherwise  $\text{VOCR}_i$  are derived from measured concentrations. In **(a)**, the red dashed line shows the fit to the acetaldehyde computed from steady-state relationships, as discussed in Appendix A.

## Temperature dependent impacts of emission controls

S. E. Pusede et al.

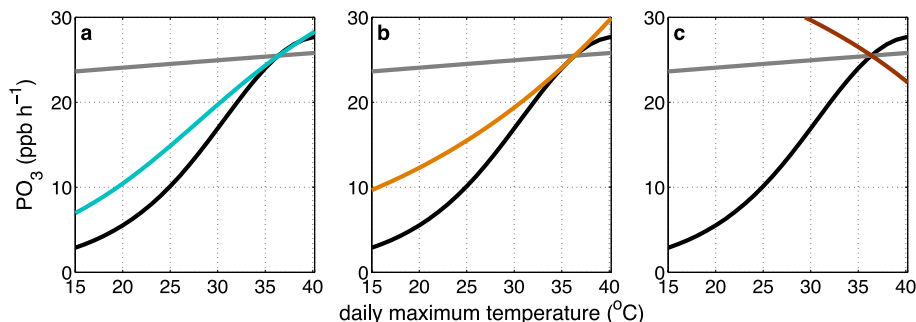


**Fig. C1.**  $PO_3$  ( $ppbh^{-1}$ ) at weekday  $NO_x$  vs. daily maximum temperature ( $^{\circ}C$ ). The solid black curves are the same as in Fig. 7a–c. The gray curves are  $PO_3$  at the high temperature average ( $36.4^{\circ}C$ ) VOCR,  $PHO_x$ , and  $NO/NO_x$  values with rate constants that are allowed to be temperature dependent. **(a)**  $PO_3$  with temperature-dependent VOCR ( $NO/NO_x$  and  $PHO_x$  are constant). **(b)**  $PO_3$  with temperature-dependent  $PHO_x$  (VOCR and  $NO/NO_x$  are constant). **(c)**  $PO_3$  with temperature-dependent  $NO/NO_x$  (VOCR and  $PHO_x$  are constant).

Title Page

Abstract

Introduction

Conclusions

References

Tables

Figures

◀

▶

◀

▶

Back

Close

Full Screen / Esc

Printer-friendly Version

Interactive Discussion

